International Journal of Applied Earth Observation and Geoinformation 125 (2023) 103566

Contents lists available at ScienceDirect

International Journal of Applied Earth Observation and Geoinformation

journal homepage: www.elsevier.com/locate/jag

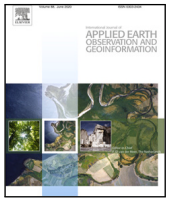

Towards intelligent ground filtering of large-scale topographic point clouds: A comprehensive survey

Nannan Qin [a], Weikai Tan [b], Haiyan Guan [a], Lanying Wang [b], Lingfei Ma [c], Pengjie Tao [d,e], Sarah Fatholahi [b], Xiangyun Hu [d,e,*], Jonathan Li [b,f,*]

[a] School of Remote Sensing and Geomatics Engineering, Nanjing University of Information Science and Technology, Nanjing, 210044, JiangSu, China
[b] Department of Geography and Environmental Management, University of Waterloo, Waterloo, N2L 3G1, Ontario, Canada
[c] School of Statistics and Mathematics, Central University of Finance and Economics, Beijing, 102206, China
[d] School of Remote Sensing and Information Engineering, Wuhan University, Wuhan, 430079, Hubei, China
[e] Hubei Luojia Laboratory, Wuhan, 430079, Hubei, China
[f] Department of Systems Design Engineering, University of Waterloo, Waterloo, N2L 3G1, Ontario, Canada

ARTICLE INFO

Keywords:
Ground filtering
Literature review
Experimental analysis
Future direction

ABSTRACT

With the fast development of 3D data acquisition techniques, topographic point clouds have become easier to acquire and have promoted many geospatial applications. Ground filtering (GF), as one of the most fundamental and challenging tasks for the post-processing of large-scale topographic point clouds, has been extensively studied but has yet to be well solved. To reveal future superior solutions, a comprehensive investigation of up-to-date GF studies is essential. However, existing GF surveys are scarce and fail to capture the latest progress and advancements. To this end, this paper not only presents a comprehensive review of up-to-date and advanced GF methods, but also conducts systematic comparative analyses of existing experimental results on public GF benchmark datasets. Moreover, this survey compiles the most recent publicly available resources that can be leveraged for the GF research, including pertinent datasets, metrics, and a range of open-source tools. Finally, the remaining challenges and promising research directions of GF, as well as implications for large-scale 3D geospatial understanding, are discussed in-depth. It is expected that this survey can simultaneously serve as a position paper and tutorial to those interested in GF.

1. Introduction

The rapid progress in 3D data collection techniques (e.g., low-cost laser scanning, depth sensors, and advanced photogrammetric reconstruction pipelines) has made point cloud acquisition more accessible and has stimulated a plethora of significant research in the domains of autonomous driving (Geiger et al., 2012), robots (Valada et al., 2017), and remote sensing (Bulatov et al., 2021). In particular, topographic point clouds over large areas have been widely used in many geospatial applications such as forest monitoring (Andersen et al., 2014; McCarley et al., 2020), archaeology (Canuto et al., 2018; Doneus et al., 2020), flood modeling (Muhadi et al., 2020), 3D urban scene interpretation (Schmohl and Sörgel, 2019), and power line corridor mapping (Ortega et al., 2019). Since raw topographic point clouds contain both the bare earth and land covers, one of the most fundamental and challenging task for the post-processing of topographic point clouds is to separate scattered points of the earth's surface into unknown ground and non-ground parts, commonly referred to as "ground filtering (GF)" (Qin et al., 2021), "bare-Earth extraction" (Sithole and Vosselman, 2004), or "point cloud filtering" (Zeybek and Şanlıoğlu, 2019).

1.1. The GF task

We assume the input is given as a 3D point cloud $PC = \{p_i | i = 1, 2, \ldots, n\}$ from the earth's surface. Each point p_i has a position $\{X, Y, Z\} \in R^3$. The primary goal of the GF task is to decompose the PC into the ground point set PS_{gr} and the non-ground point set PS_{ng}. PS_{gr} usually contains the bare terrain (e.g., top soil and water surface), or any impervious surface covering it. PS_{ng} typically represents the objects above the ground surface (e.g., roofs, vegetation, cars, etc.), as well as possible low or high outliers.

1.2. Challenges

In light of the above task concern, a discriminate and general-purpose GF algorithm should be: (1) able to handle the terrain details;

* Corresponding author at: School of Remote Sensing and Information Engineering, Wuhan University, Wuhan, 430079, Hubei, China.
E-mail addresses: huxy@whu.edu.cn (X. Hu), junli@uwaterloo.ca (J. Li).

https://doi.org/10.1016/j.jag.2023.103566
Received 21 September 2023; Received in revised form 9 November 2023; Accepted 10 November 2023
Available online 21 November 2023

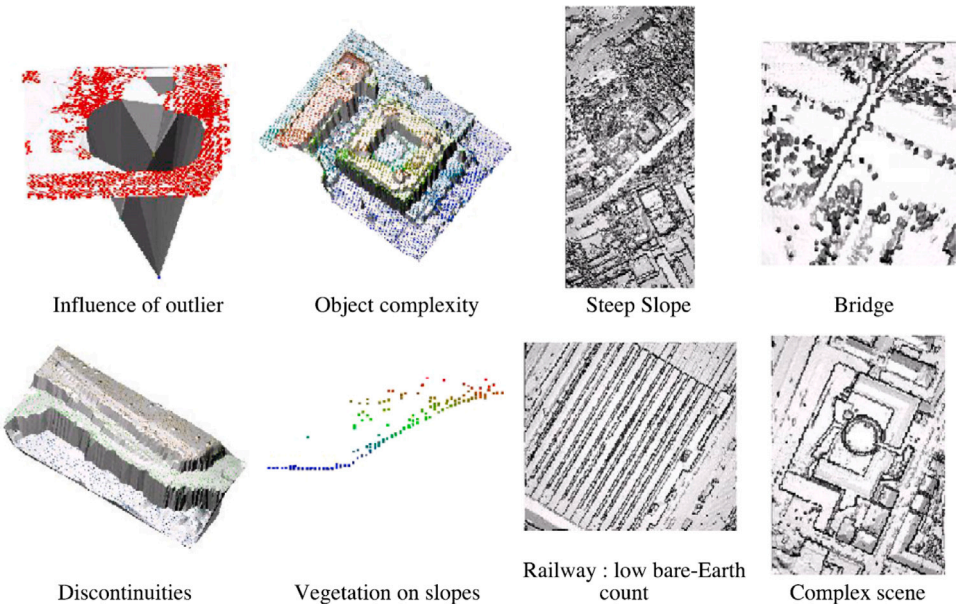

Fig. 1. Typical difficulties in the GF task.
Source: Adapted from Sithole and Vosselman (2004), Fig. 2.

(2) robust for different landscapes; (3) capable of handling large-scale point clouds; (4) acceptable in regard to the memory and computation costs. However, different from indoor scenes, the outdoor earth's surface covers various complex objects and terrains, posing great challenges to GF algorithms. For one thing, the significant topographic fluctuation changes and complex structures of objects generate pronounced distinctions within the class *ground/non-ground*; for another, the *ground* and *non-ground* categories often exhibit remarkably similar geometric structures.

Specifically, the main difficulties in the GF task include: (1) outliers under/above the ground; (2) objects with large coverage (e.g., large buildings); (3) objects close to the ground (e.g., bridges connected to the ground, slow vegetation above high relief areas, short walls, fences beside the road); (4) areas with dense vegetation and sharply changing topography (e.g., cliffs, shores, and riverbanks); (5) mixed areas characterized by low and high slopes (e.g., slope areas with scatted buildings); (6) disconnected terrain (e.g., jagged hilly edges). Several typical examples are shown in Fig. 1.

Furthermore, even if the classification accuracy is very high, the extracted ground surface may not describe the real world as realistically as expected, owing to the missing of a small number of key ground points (e.g., mountain ridge/valley points) or the residual of a small number of low object points (e.g., vegetation points close to the slope).

1.3. Motivation

Over the last few decades, numerous algorithms have been developed to tackle the aforementioned challenges. Early GF methods belong to unsupervised knowledge-driven techniques, which heavily rely on geometric priors. As the geometric priors are common knowledge and contain less ambiguous judgments, these methods have high stability and certainty in some specific scenes. However, they are challenging to strike a balance between the detail preservation and filtering effectiveness when processing complex scenes. More recently, data-driven pipelines operating under supervised learning paradigms, particularly those utilizing deep learning (DL) techniques, have demonstrated encouraging GF performances in challenging terrains. Nevertheless, these supervised end-to-end pipelines often suffer from overfitting to the data distribution of training samples and have poor interpretability on their errors. Therefore, some practical applications (e.g., civil engineering and disaster response) that require high stability cannot fully trust them.

Due to the advantages and disadvantages of the above two kinds of methods, unsupervised ground filters are still being studied apart from advanced DL-based GF pipelines. This makes us confused about the future direction of GF research, and brings us a series of fundamental questions: (1) Why are there so many branches of mathematical and computational methods designed to solve the GF problem? (2) Is it still necessary to conduct further in-depth research on GF? (3) Is relying solely on cutting-edge theories and technologies in relevant fields sufficient to address the remaining challenges of GF research?

Answering these questions requires not only in-depth principle analyses of existing methods, but also systematic experimental comparisons on well-recognized datasets. Existing GF investigations, however, focus only on either the literature review or the experimental comparison (Liu, 2008; Meng et al., 2010; Chen et al., 2017; Sithole and Vosselman, 2004; Korzeniowska et al., 2014; Luis Montealegre et al., 2015; Stereńczak et al., 2016; Zhao et al., 2018; Silva et al., 2018; Serifoglu Yilmaz et al., 2018; Serifoglu Yilmaz and Gungor, 2018; Jakovljevic et al., 2019; Klápště et al., 2020; Moudry et al., 2020; Chen et al., 2021), especially lacking the latest progress of advanced DL techniques in GF. To promote the advancement of more intelligent GF solutions, a large-scale GF benchmark dataset and extensive experimental evaluations have been introduced in our previous works (Qin et al., 2021, 2023). In this paper, we focus on going through a comprehensive GF survey by presenting an up-to-date literature review, summarizing representative experimental evaluations, compiling publicly available resources, clarifying remaining key challenges, and suggesting promising directions for future research.

1.4. Contributions

We believe our work would benefit both academic communities and industrial applications. The main contributions of this paper include:

- Presenting a comprehensive literature review of the up-to-date progress on GF. To the best of our knowledge, it is the first survey systematically covering advanced DL-based GF methods.
- Conducting systematic comparative analyses of existing experimental results evaluated on public GF benchmark datasets.

Table 1
Representative 3D geospatial datasets for GF.

Dataset	Year	Area	Points	Publicly available	Scene
ISPRS-Filtertest (Sithole and Vosselman, 2003)	2003	1.1×10^6 m^2	0.4 M	Yes	multiple
OpenGF (Qin et al., 2021)	2021	47.7×10^6 m^2	542 M	Yes	multiple
SC (Hu and Yuan, 2016)	2016	235×10^6 m^2	94 M	No	multiple
FE (Jin et al., 2020)	2020	5×10^6 m^2	51 M	Yes	single

- Delineating several promising GF research directions, in response to the remaining key challenges. Some implications for large-scale 3D geospatial understanding are also revealed.
- Delivering the latest public resources that can be exploited for GF research, including relevant datasets, metrics, and open-source tools.

Following the introduction part in Section 1, the subsequent parts of this paper are structured as follows. A summary of the existing datasets and evaluation metrics for GF is introduced in Section 2. In Section 3, an exhaustive review of existing GF approaches is provided. Section 4 lists available open-source tools for GF. Systematic comparisons of experimental results on public GF benchmark datasets are conducted in Section 5. Section 6 discusses the remaining challenges and promising research directions of GF, as well as implications for large-scale 3D geospatial understanding. We finally conclude this survey in Section 7.

2. Existing datasets and metrics

2.1. Datasets for GF

With the growing utilization of LiDAR in a variety of fields, including autonomous driving and remote sensing, the number of large-scale datasets containing millions of points is on the rise. These datasets have been instrumental in contributing to the development of data-driven DL pipelines for 3D point cloud semantic labeling.

According to different data collection techniques, current 3D geospatial point cloud datasets can be broadly categorized into three groups. (1) Photogrammetric 3D point cloud datasets (Li et al., 2020; Hu et al., 2022). These datasets are generated using passive photogrammetry techniques. Owning to the absence of ground points within areas covered by dense vegetation, they have inherent limitations in training DL-based GF models in forest regions. (2) Terrestrial laser scanning/Mobile laser scanning (MLS) point cloud datasets (Hackel et al., 2017; Roynard et al., 2018; Behley et al., 2019; Tan et al., 2020). These datasets are typically acquired at the street level to enhance understanding of roadway scenes. Limited by the spatial coverage, these datasets are not well-suited for the GF of large regions. (3) Airborne laser scanning (ALS)/Unmanned aerial vehicle laser scanning (UAV-LS) point cloud datasets (Niemeyer et al., 2014; Zolanvari et al., 2019; Ye et al., 2020; Varney et al., 2020; Kölle et al., 2021). These datasets are commonly acquired for the purpose of 3D urban perception. They prioritize the identification of various objects above the ground (e.g., trees, buildings, fences, and bridges) over accurate ground extraction. Additionally, such datasets provide limited coverage of common non-urban landscapes, such as forests and mountains.

To the best of our knowledge, there are primarily two categories of datasets used to evaluate GF methods. The first type consists of public benchmark datasets, such as the ISPRS-Filtertest dataset (Sithole and Vosselman, 2003) and the OpenGF dataset (Qin et al., 2021). The second type consists of experimental datasets employed in recent studies that investigate DL-based GF methods, e.g., the South China (SC) dataset used in Hu and Yuan (2016), the Forest Environment (FE) dataset used in Jin et al. (2020), and the UAV-LS dataset used in Li et al. (2022). A comprehensive comparison of representative 3D geospatial datasets for GF is presented in Table 1, and the specific descriptions are as follows:

ISPRS-Filtertest[1] (Sithole and Vosselman, 2003). It contains a set of point clouds collected by an Optech ALTM scanner from different regions with diverse characteristics. The test set consists of eight sites, with four representative urban landscapes and the other four representative rural landscapes. Among these eight sites, two of them were provided at reduced densities to enable the evaluation of filtering performance across varying point cloud densities. In addition, 15 reference samples were labeled through a process of semi-automatic filtering and manual editing. Leveraging the reference data, researchers can undertake experimentation, assessment, and comparison of their own algorithms with existing other methods. Since 2003, this dataset has emerged as a pivotal source for conducting GF experiments.

OpenGF[2] (Qin et al., 2021). It is the first ultra-large-scale public dataset dedicated to developing advanced DL methods for GF. OpenGF contains over 542 million points covering more than 47 km^2 of area. A total of 160 point cloud tiles were carefully chosen as the training set from four primary terrain scenes, namely, Metropolis, Small City, Village, and Mountain. Each tile covers 500×500 m^2. Among these 160 tiles, nine representative tiles were chosen for validation. Besides, three additional challenging point clouds characterized by hybrid terrain scenes, objects in various sizes, and terraced slopes, were selected as the test set.

SC (Hu and Yuan, 2016). It contains 900 ALS point cloud tiles in South China for training models. Each tile covers 500×500 m^2 with an average point density of 4 pts/m^2. 40 additional point cloud tiles including about 40 million points were used as the test set. The ground truth labels of the training and test sets were generated through a process of semi-automatic filtering and manual editing.

FE[3] (Jin et al., 2020). It comprises a total of 20 ALS point cloud tiles, which were selected from four distinct study regions with significant variations in both topography and vegetation of the Southern Sierra Nevada Mountains, CA, USA. Each tile covers 500×500 m^2. The point clouds were obtained during August 2010 utilizing an Optech ALTM scanner, with an average point density of approximately 10.27 pts/m^2. There are 14 point clouds in this dataset designated as the training set, which exhibits different ranges of canopy cover and slope. It is noteworthy that the authors originally developed this dataset for their own research purposes and subsequently have made it available to the public.

2.2. Evaluation metrics for GF

Earlier studies usually tested their GF approaches using the conventional metrics from the ISPRS-Filtertest benchmark dataset (Sithole and Vosselman, 2004). These metrics (i.e., Type I error, Type II error and Total error) were computed through the generation of cross-matrices. To enhance accessibility for researchers in related fields, Qin et al. (2021) have substituted these traditional metrics with comparable alternatives (i.e., IoU_1, IoU_2, OA) that are presently popular in semantic segmentation tasks. The filtering performance was also evaluated with the root mean square error ($RMSE$) between the generated digital

[1] https://www.itc.nl/isprs/wgIII-3/filtertest
[2] https://github.com/Nathan-UW/OpenGF
[3] https://3decology.org/2023/06/21/benchmark-dataset-for-airborne-lidar-scanning-data-filtering-in-forested-environments-2/

Table 2
Exemplary metrics employed in public GF benchmark datasets.

Metric	Equation	Description	
Type I error	$\frac{FP_2}{TP_2+FP_2}$	The proportion of misclassified ground points	TP_1, FP_1, TP_2, and FP_2 are, respectively, the number of correctly identified non-ground points, the number of non-ground points erroneously classified as ground points, the number of correctly identified ground points, and the number of ground points erroneously classified as non-ground points
Type II error	$\frac{FP_1}{FP_1+TP_1}$	The proportion of misclassified non-ground points	
Total error	$\frac{FP_1+FP_2}{TP_1+FP_1+TP_2+FP_2}$	The proportion of all the misclassified points	
IoU_1	$\frac{TP_1}{TP_1+FP_1+FP_2}$	The intersection over union of class non-ground	
IoU_2	$\frac{TP_2}{TP_2+FP_2+FP_1}$	The intersection over union of class ground	
OA	$\frac{TP_1+TP_2}{TP_1+FP_1+TP_2+FP_2}$	Overall accuracy	
$RMSE$	$\sqrt{\frac{\sum_{i=1}^{N}(G_i-R_i)^2}{N}}$	The root mean square error between the generated DTM and the reference DTM	G_i and R_i denote the valid elevation value of the generated DTM and the reference DTM, respectively. N represents the total number of pixels with a valid elevation value

DTM denotes digital terrain model.

Table 3
Summary of typical GF methods.

	Typical method	Pioneering work	Main advantage	Main limitation
Unsupervised	Morphology-based	Kilian et al. (1996)	Work well in rugged areas with high efficiency	Unsuitable for terrains with diverse objects
	Surface-based	Kraus and Pfeifer (1998)	Effective in most terrains	Unsatisfied performance in handling terrain details
	Slope-based	Axelsson (2000)	Work well in flat areas with high efficiency	Unsuitable for terrains with abrupt changes
	Cluster-based	Tóvári and Pfeifer (2005)	Effective in terrains with diverse objects	Limited by the segmentation performance
	Statistic-based	Bartels and Wei (2006a)	Effective in flat terrains without diverse objects	Low reliability in complex terrains
Supervised	RML-based	Lu et al. (2009)	More flexibly in complex terrains	Limited by the hand-crafted features
	DL-based	Hu and Yuan (2016)	High classification accuracy in complex terrains	Unsatisfied performance in challenging local areas

RML and DL denote regular machine learning and deep learning, respectively.

terrain models (DTMs) and the reference DTMs (Hu and Yuan, 2016; Qin et al., 2021, 2023). In addition, several classical classification metrics (e.g., *precision*, *recall*, $F1$-score) have been employed directly in recent GF studies (Nurunnabi et al., 2021; Li et al., 2022). These metrics are also important besides OA and $RMSE$, especially in different terrain conditions. Table 2 enumerates several metrics employed in existing public GF benchmark datasets.

3. Literature review

In this section, we review the concepts, advantages, and limitations of existing GF methods in detail. These approaches are mainly designed for ALS point clouds, and many of them can also be applicable to photogrammetric point clouds or even MLS point clouds (Gomes et al., 2023). According to different principles adopted, they can be classified into two primary groups (i.e., unsupervised and supervised) and seven representative sub-groups. The advantages and limitations of typical GF methods are summarized in Table 3. Overall, different types of GF methods have their own pros and cons, which are discussed in detail at the end of corresponding sections. In addition to these typical methods, several hybrid GF methods (Hou et al., 2014; Guan et al., 2014; Zhao et al., 2016; Yang et al., 2016; Kumar et al., 2018; Ma and Li, 2019; Cai et al., 2019; Hui et al., 2021; Bulatov et al., 2021; Štroner et al., 2021) were also proposed.

Fig. 2 is a stacked bar chart which shows the trends in the number of existing publications on GF since 1996 to our best knowledge. It can be observed that: (1) The number of publications on GF shows a trend of overall growth over time. (2) Before 2016, almost all GF methods were unsupervised. Among these methods, surface-based GF methods were the most widely studied. (3) 2018 was the year with the highest number of publications, and the types of methods used in these publications were also the most diverse. Since then, the research on DL-based GF methods has become a new hotspot and has gained the most attention from researchers.

3.1. Unsupervised ground filters

Unsupervised ground filters are usually built based on hand-crafted geometric/statistical constraints, and do not require additional supervised information. As shown in Table 3, they can be categorized into five groups: (1) Morphology-based filters, (2) Surface-based filters, (3) Slope-based filters, (4) Cluster-based filters, and (5) Statistic-based filters.

3.1.1. Morphology-based filters

Morphology-based filters usually operate morphological operations (e.g., erosion, dilation, and opening) to filter non-ground points within a local window (see Fig. 3).

The initial utilization of a simple opening operation to separate non-ground points from ground points was demonstrated by Kilian et al. (1996). Due to the use of relatively small structural elements, this method cannot successfully filter out large-sized objects such as buildings and dense forests (Zhang et al., 2003). To solve this problem, studies tried to apply a progressive strategy. For instance, a

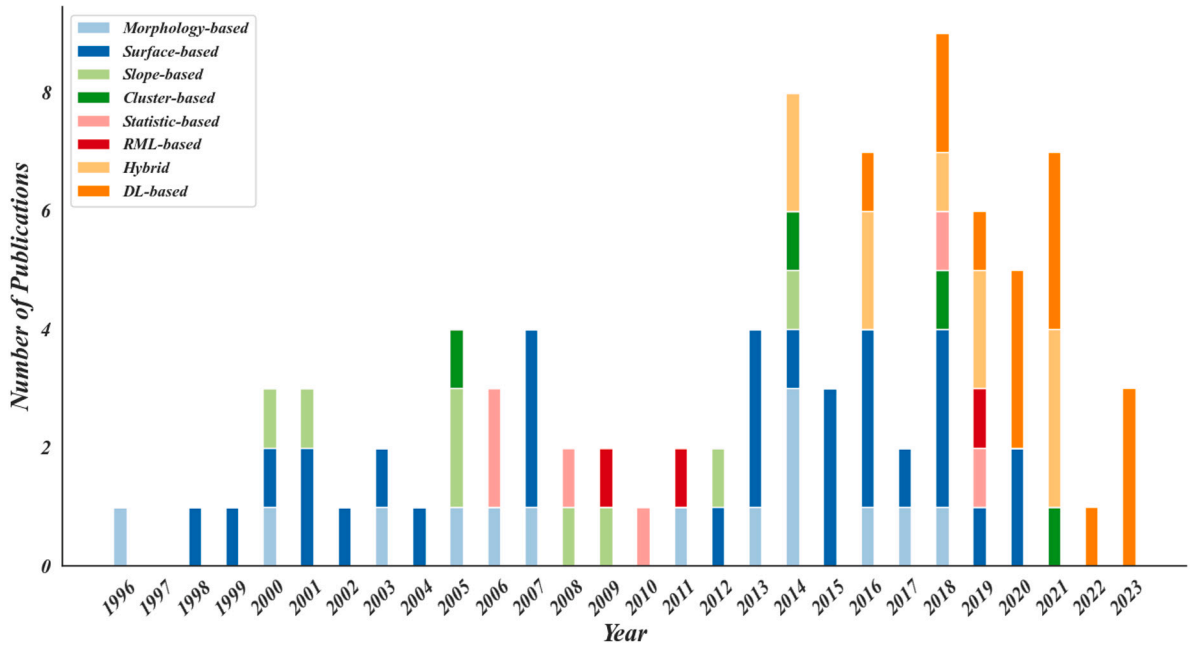

Fig. 2. Trends in the number of publications on GF.

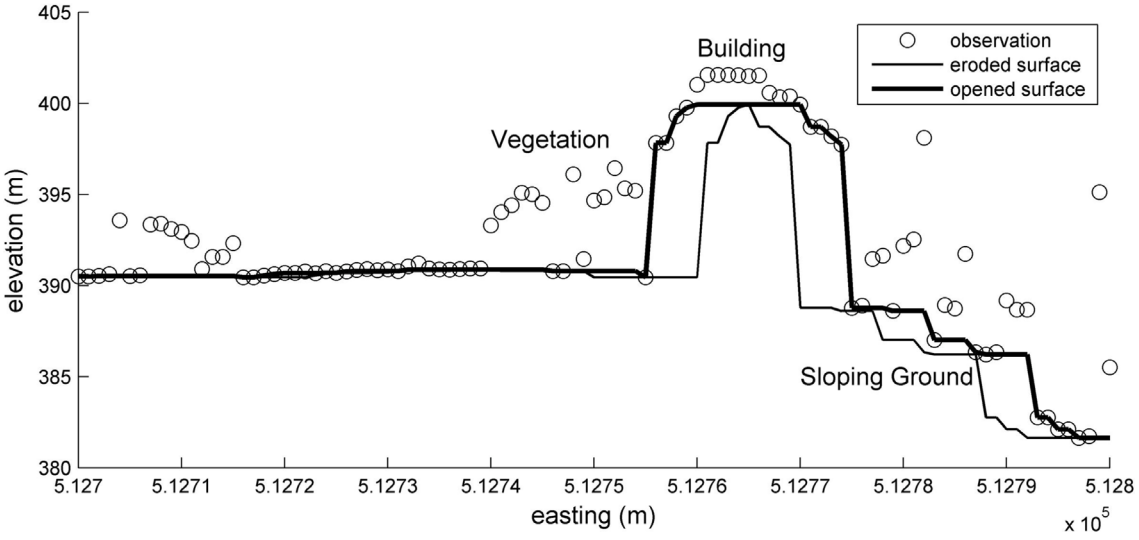

Fig. 3. An example of the morphology-based filter.
Source: Adapted from Pingel et al. (2013), Fig. 2.

progressive morphological filter (PMF) was employed by Zhang et al. (2003), which gradually raised the window size. Chen et al. (2007) also employed a progressively increasing window size for morphological operations. Unlike Zhang et al. (2003), this approach does not assume a constant slope. Pingel et al. (2013) proposed a simple morphological filter called SMRF, which adopted a linearly increasing window size and a slope threshold to remove non-ground points. The ground extraction method proposed by Mongus et al. (2014) involves thresholding from differential morphological profiles built from the point residuals. Mongus and Žalik (2014) proposed a morphological filter that utilizes some connected operators and multi-scale decomposition to achieve computational efficiency. Hui et al. (2016) integrated the PMF with multi-level interpolation filtering to preserve abrupt terrain features. Arefi and Hahn (2005) presented a method that combined gray-scale morphological reconstruction and geodesic filtering to separate ground points from non-ground points without setting a specific kernel size. Lohmann et al. (2000) proposed a dual rank filtering approach by combining gray-scale erosion and dilatation operations with a small mask, which showed a reliable recognition and removal of the artificial structures. Liu and Lim (2018) proposed a voxel-based multi-scale morphological filtering method for the forest region, which takes advantages of the height distribution of the points and height difference of surrounding points. The approach proposed by Li et al. (2011) involves the initial detection of edge points corresponding to vegetation and buildings, followed by the application of an opening operation to the remaining points in the local region, which effectively preserves terrain details. Li et al. (2017) introduced a GF method utilizing geodesic transformations of mathematical morphology, which aims to address the issue of structuring element selection dependency. In addition, some studies have sought to improve the effectiveness of morphology-based methods in complex terrains. For instance, Zakšek et al. (2006) developed an improved morphological filter specifically designed for areas characterized by steep terrain and dense vegetation. Li et al. (2014) proposed an enhanced morphological top-hat

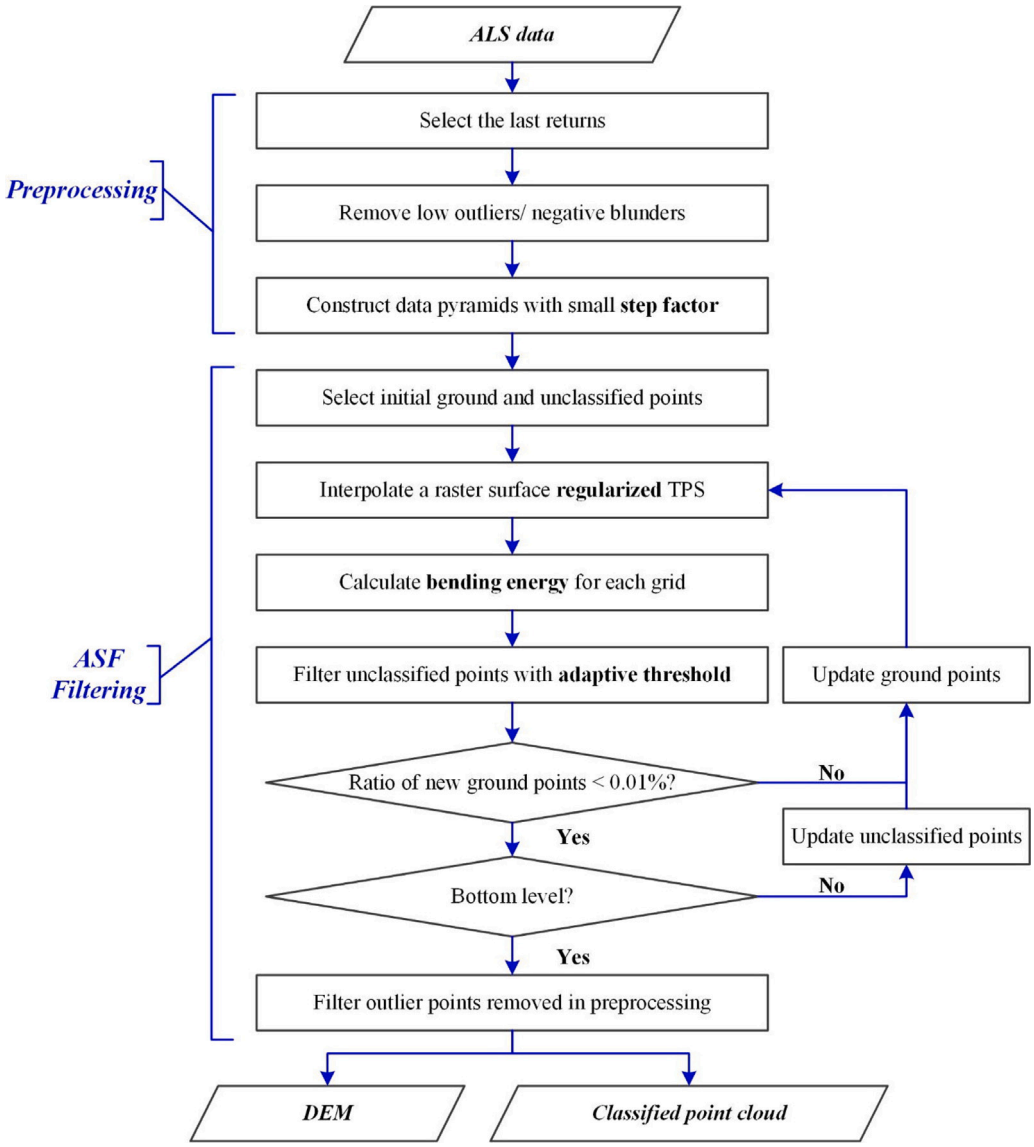

Fig. 4. An example of the interpolation-based filter.
Source: Adapted from Hu et al. (2014), Fig. 2.

filter that incorporates a slope brim to separate ground points from non-ground points, which has demonstrated effectiveness in processing rugged terrains with complex objects.

Although morphology-based filters have demonstrated robustness in rugged regions and effectiveness in removing small objects, their performance may be unsatisfactory in terrains with a variety of objects.

3.1.2. Surface-based filters

Surface-based filters first construct a reference surface by discriminant functions, and then determine the point category by the spatial distance between each point and the corresponding reference surface. According to different reference surface generation methods, such filters can be categorized into three groups: (1) Interpolation-based filters, (2) Triangular-irregular-network (TIN)-based filters, and (3) Contour-based filters.

Interpolation-based filters. In interpolation-based filters, the reference ground surface is interpolated from initially selected ground seed points and gradually refined with newly selected ground points (see Fig. 4).

Earlier linear-prediction-based filters involve the computation of mean elevation values to construct the initial surface, and iterative refinement of the ground surface by assigning appropriate weights to each point (Kraus and Pfeifer, 1998; Pfeifer et al., 1999; Kraus and Pfeifer, 2001). Such methods tend to perform satisfactorily in most terrain scenes but may misclassify small non-ground objects. Lee and Younan (2003) introduced a modified linear prediction method that improves the GF performance in significant variable terrains through adaptive processing. Crosilla et al. (2004) also proposed an efficient GF approach that relied on a novel tool for carrying out robust regression and estimation of location and shape. In order to enhance the accuracy of reference ground surfaces, many researchers have suggested the use of methods employing multi-scale interpolation with nonlinear interpolators. One such approach, proposed by Pfeifer et al. (2001), involves the incorporation of a linear-prediction-based filter (Kraus and Pfeifer, 1998) into a hierarchical structure. Another representative method, developed by Evans and Hudak (2007), is the multi-scale curvature classification (MCC) method for GF, which employs thin plate spline (TPS) interpolation to the seed points to generate a reference ground surface. Chen et al. (2013) proposed a hierarchical approach that entails a progressive increase in cell size and residual threshold at different resolution levels. In this method, the generated surface using TPS is subject to iterative updates. Hu et al. (2014) enhanced

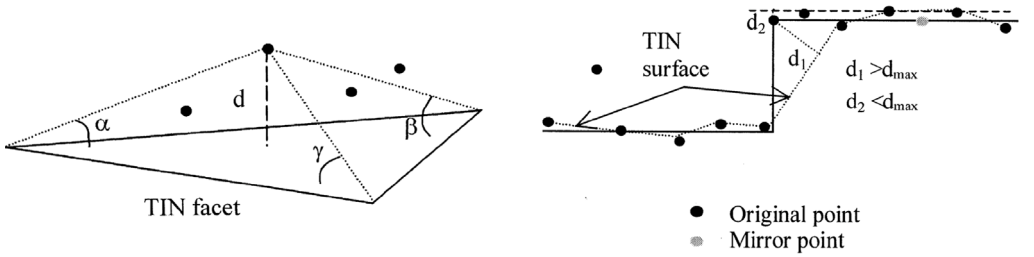

Fig. 5. An example of the TIN-based filter.
Source: Adapted from Axelsson (2000), Figs. 3 and 4.

this method by incorporating a smoothing TPS between adjacent levels with a step size of less than two. In addition, Liu et al. (2020) proposed a saliency-aware TPS interpolation to achieve a terrain-adaptive GF method.

Mongus and Žalik (2012) introduced a parameter-free method for the GF of LiDAR point clouds using a hierarchical TPS interpolation. In this method, a top-hat transformation is employed to amplify the discontinuities in terrain caused by objects. Additionally, a parameter-free filtering technique is introduced, which utilizes an automatic thresholding method based on standard deviation. Abdeldayem (2019) proposed a GF approach that utilizes an automatic weighted splines filtering algorithm. This method involves the utilization of cubic smoothing splines for interpolating raw point clouds. For the steep and forested terrains, Kobler et al. (2007) proposed a repetitive interpolation filtering workflow with an initial filtering step to eliminate low outliers and the majority of non-ground points. Similarly, Maguya et al. (2013) proposed an adaptive interpolation method by identifying complex terrain types. Su et al. (2015) proposed a GF method involving a hierarchical moving curve-fitting filter, which utilizes flexible tiles of moving blocks to fit a second-degree polynomial surface. In addition, Nurunnabi et al. (2015) introduced a GF approach based on robust locally weighted regression. Qin et al. (2017) used second-order polynomial fitting as a means of selecting ground points, and applied the region-growing algorithm to expand upon the selection. Zheng et al. (2007) proposed a fast facet-based GF method that employs simple, quadratic, and cubic facet models.

TIN-based filters. In TIN-based filters, a coarse TIN is firstly constructed with local lowest points as the reference ground surface, additional ground points are then classified and added to this TIN to progressively densify the triangulation (see Fig. 5).

The progressive TIN densification (PTD) method (Axelsson, 2000), known for its robustness, has gained significant attention and has been widely adopted in commercial software. However, the PTD method is often time-consuming because of the iterative TIN construction (Chen et al., 2016a). To obtain better performance, many different optimization solutions for the PTD method have been proposed. For example, Zhang and Lin (2013) first selected some seed ground points for initial TIN construction, and then applied a region-growing approach to gradually densify the TIN surface. Dong et al. (2018) improved the PTD method to handle higher density point clouds with high standard variance by using a two-stage densification strategy. Chen et al. (2016a) proposed three strategies to overcome difficulties in mountain ridges by introducing the ridge triangle, optimal selection strategy, and stopping criterion of the TIN densification step, which works well in urban and mountain areas. Shi et al. (2018) proposed a parameter-free version of the PTD algorithm, which aims to address the sensitivity of the classic PTD algorithm to the maximum angle and distance.

Contour-based filters. In contour-based filters, active shape models are utilized to represent the reference ground contour/surface. The contour function behaves akin to a mesh, progressively eliminating non-ground points through the utilization of force measurements like gravity and attraction (see Fig. 6).

Elmqvist (2002) first proposed a GF method based on active shape models, with the energy function being a weighted combination of both internal and external forces. Similarly, Zhang et al. (2016) introduced a cloth simulation filtering (CSF) method that has several easy-to-set parameters. This method first flips the point cloud upside-down and covers it with a rigid cloth, then shifts the nodes of the cloth by calculating the interactions with the corresponding local points, finally determines the ground points by comparing the input point cloud with the corresponding generated surface. Yang et al. (2020) proposed a bidirectional CSF method combining forward and inverse filtering, which outperforms the CSF method significantly when dealing with airborne LiDAR bathymetry point clouds. Hu et al. (2015) introduced a computationally efficient algorithm named semi-global filtering that constructs a unique energy function. In addition, Ural and Shan (2016) proposed a GF method that utilizes minimum cut to minimize the energy function where both global and local features are taken into consideration. Similarly, He et al. (2018) employed a progressive GF approach using graph cuts.

The surface-based filters have been extensively adopted and have yielded satisfactory performance in most landscapes. Nevertheless, these approaches may encounter challenges in preserving terrain details and may misclassify small objects near the ground.

3.1.3. Slope-based filters

Slope-based filters extract the ground based on the disparity in slope between two points. If the slope is larger than a specific threshold, the higher point will be categorized as *non-ground* (see Fig. 7).

The classic slope-based filter was first proposed by Vosselman (2000) based on assessing the local maximum slope. Since this method is greatly influenced by the actual slope and elevation difference of the landscape, it is unsuitable for deployment in complex terrains. In order to adapt the slope threshold to complex terrains, Sithole (2001) suggested an improved slope-based approach which calculates the slope threshold from local point clouds. Susaki (2012) proposed an iterative GF method and the slope threshold is updated automatically after each iteration. To improve efficiency, Shan and Aparajithan (2005) utilized the scan line information and calculated slope parameter based on a 1D point cloud profile. However, the fixed slope threshold is unsuitable for large relief areas with dense coverage. To solve this kind of issue, Shao and Chen (2008) employed three slope parameters for searching the ground points, namely the general slope, slope increment, and maximum slope. Meng (2005) proposed a multi-directional filter based on the accumulated calculation results of the slope change and the local elevation difference, which has better results in small hill areas. This method was subsequently improved by incorporating a 2D neighborhood and utilizing pattern features of different directions across the rasterized point clouds (Meng et al., 2009). In addition, to solve the over-filtering problem, Wang and Tseng (2014) integrated the

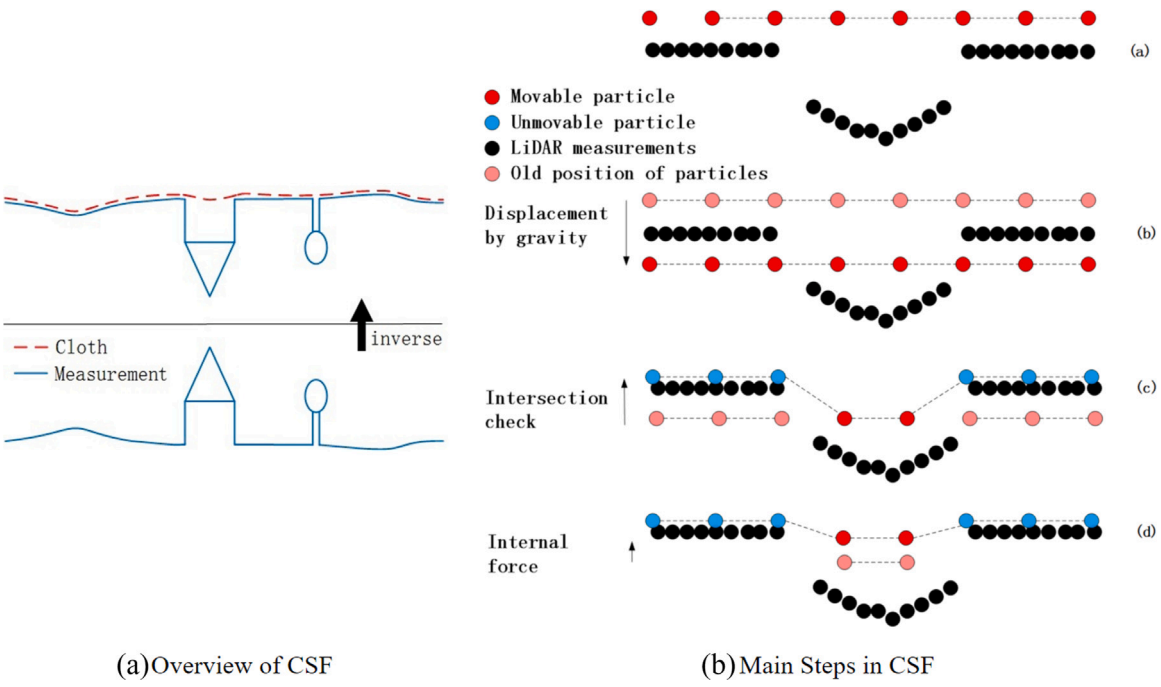

Fig. 6. An example of the contour-based filter. *Source:* Adapted from Zhang et al. (2016), Figs. 1 and 3.

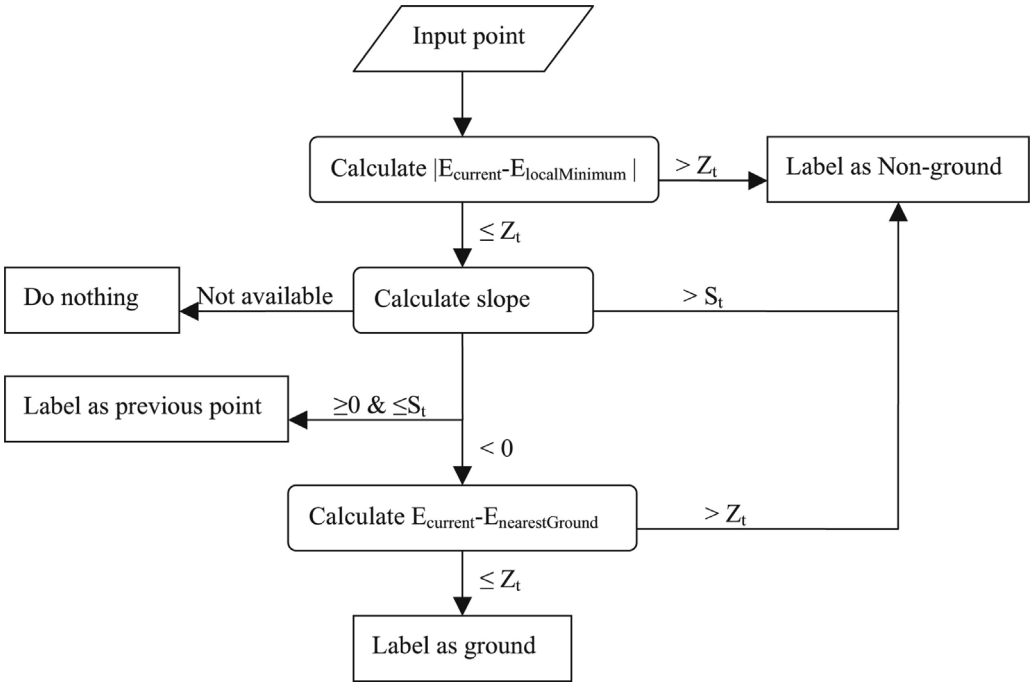

Fig. 7. An example of the slope-based filter. *Source:* Adapted from Meng et al. (2009), Fig. 1.

adaptive slope and directional filtering concepts into a dual-directional slope-based filter.

Slope-based filters possess an inherent advantage in their simplicity and superior computational efficiency. However, these filters are often sensitive to the parameters used, especially in steep mountainous regions with abrupt changes.

3.1.4. Cluster-based filters

Cluster-based filters first generate similar point cloud patches using clustering/segmentation methods, and then extract the ground segments based on geometric and topological information (see Fig. 8).

Sithole and Vosselman (2005) utilized the scan line segmentation with multiple orientations to separate the original point cloud into a set

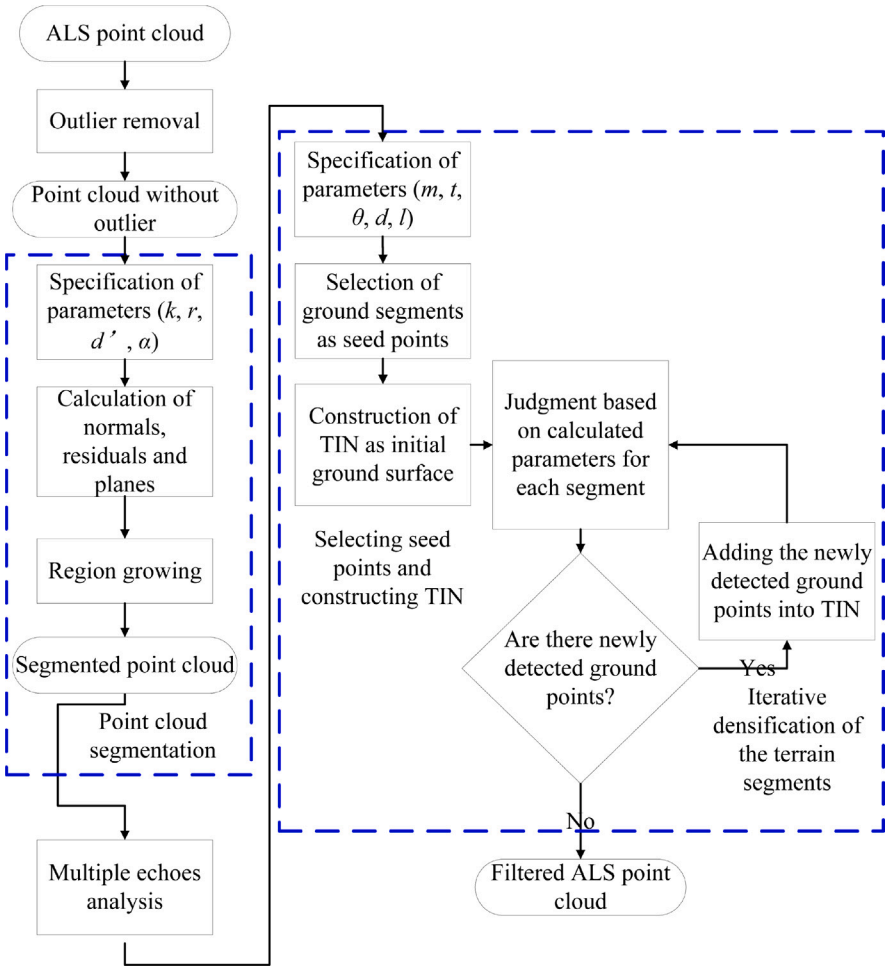

Fig. 8. An example of the cluster-based filter.
Source: Adapted from Lin and Zhang (2014), Fig. 2.

of smooth segments. The segments were then classified into ground or non-ground surfaces according to the geometric relationships with the neighbors. Lin and Zhang (2014) first segmented the input point cloud, then analyzed the echo information to eliminate vegetation points, and finally extracted ground segments based on the classic PTD method. Ni et al. (2018) utilized a combination of clusters and iterative graph cuts to identify ground points. This method initially generates clusters from raw point clouds with a two-step clustering method, and subsequently extracts the ground at the cluster level. Che et al. (2021) extracted the ground from large-scale point clouds based on multi-scale voxelization and smooth segments.

Although cluster-based approaches can partially retain terrain discontinuities and withstand anomalies, their effectiveness is highly dependent on the performance of the segmentation operation.

3.1.5. Statistic-based filters

Statistic-based filters typically suppose that the ground elevation conform to a particular distribution, while the presence of objects may disrupt this distribution (see Fig. 9).

Bartels and Wei (2006a) first presented a GF method, named skewness balancing, by exploiting measures of distribution. This method was further extended with a prediction module that classifies point cloud tiles as either hilly or flat terrain types (Bartels and Wei, 2010). The extended method remains threshold-free and is indifferent to LiDAR data format and resolution. Bao et al. (2008) also introduced a statistical algorithm designed to differentiate ground points from non-ground points in mountainous regions. This approach predicates ground points by the skewness change of point intensity. Hui et al. (2019) also proposed a threshold-free GF method based on the expectation maximization algorithm. In addition, Bartels and Wei (2006b) proposed a wavelet-based GF method for hilly terrains. However, this approach failed for large flat roofs and attached objects such as bridges. Bayram et al. (2018) presented a spectral graph filtering algorithm for LiDAR point clouds. This algorithm processes 3D point clouds on their original domains by interpreting them as elevation signals of weighted graph representations.

Statistic-based filters typically perform well in flat terrain without complex objects. However, the reliability of these methods may significantly reduce in complex terrains.

3.2. Supervised learning-based pipelines

Learning-based pipelines formulate the GF task as a binary probability classification problem. They take advantage of sufficient labeled samples and advanced learning techniques to extract the ground from challenging and complex point clouds. Currently, the adopted supervised learning techniques in GF studies can be divided into two types: (1) Regular machine learning (RML) and (2) DL.

3.2.1. RML-based pipelines

Early RML-based pipelines leveraged diverse conventional classifiers to learn discriminant rules directly from handcrafted features. Lu

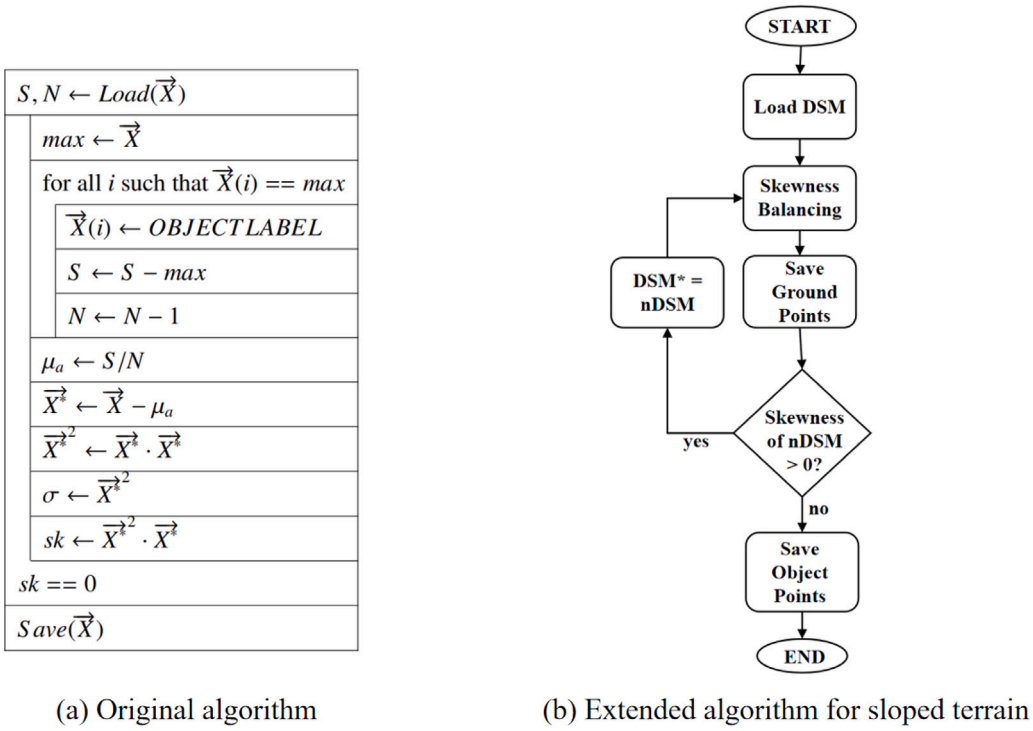

(a) Original algorithm (b) Extended algorithm for sloped terrain

Fig. 9. An example of the statistic-based filter.
Source: Adapted from Bartels and Wei (2010), Fig. 1.

et al. (2009) used hand-crafted features and hybrid conditional random fields for ground extraction. Jahromi et al. (2011) proposed a GF method based on artificial neural networks. In addition, methods using hand-crafted features and support vector machines were also developed (Ayazi and Saadat Seresht, 2019).

While RML-based pipelines afford relatively flexible handling of complex scenes, their GF performance is ultimately constrained by the hand-crafted features.

3.2.2. DL-based pipelines

The utilization of implicit features learned by deep neural networks (DNNs) can lead to superior GF performance in comparison to hand-crafted features, which have a lower level of descriptiveness. Depending on different data formats fed into DNNs, existing DL-based GF pipelines can be categorized into three groups: (1) 2D-image-based pipelines, (2) 3D-voxel-based pipelines, and (3) 3D-point-based pipelines.

2D-image-based pipelines. In 2D-Image-based pipelines, the generation of feature maps and the construction of deep architectures are two pivotal modules. Initially, hand-crafted features are employed for generating structured 2D feature maps. Once the points are projected into 2D feature maps, well-engineered 2D DL models can be directly utilized for subsequent processing (see Fig. 10).

Hu and Yuan (2016) first proposed a GF method by adopting 2D deep convolution neural networks (DCNNs), and obtained significantly better results than traditional ground filters on the ISPRS-Filtertest dataset, which provides a new idea for GF. However, this method loses some vertical structure information during the process of converting 3D point clouds to 2D feature maps, resulting in poor filtering performance in complex mountain areas. In addition, due to the point-wise classification strategy, the processing efficiency of this method is low (Rizaldy et al., 2018). To solve these problems, an improved method based on a 2D semantic segmentation network was proposed by Rizaldy et al. (2018). First, the original point cloud is mapped into a multi-channel feature map, then the feature map is classified with 2D full convolution neural networks (FCNs) (Shelhamer et al., 2017), and finally, the classification result of the feature map is mapped back to the point cloud. Similarly, Gevaert et al. (2018) proposed a GF method with 2D FCNs for the photogrammetric point cloud. However, it is difficult to get ideal classification results by using 2D FCNs to deal with a projection map with serious overlap between the ground and non-ground areas.

3D-voxel-based pipelines. In addition to the 2D-image representation, the 3D-voxel representation is another solution for using well-engineered CNN architectures directly. In 3D-voxel-based pipelines, point clouds are first voxelized, and features are then calculated from the voxel grids (see Fig. 11).

Yotsumata et al. (2020) first employed the dense 3D CNN for the GF of voxelized point clouds. Subsequently, Dai et al. (2023) proposed a novel 3D-voxel-based GF pipeline based on MinkUNet (Choy et al., 2019), which aims to achieve a high voxel resolution while simultaneously capturing extensive spatial contextual information. The advantage of these pipelines is that they can retain approximately 3D structural information and apply 3D convolution operations directly. However, the 3D-voxel-based pipelines incurs quantization losses during the process of obtaining a voxel grid, which is contingent upon the size of the 3D voxel unit. Moreover, conflicts between resolution and sampling extent can result in the misclassification of micro-terrain details or large objects.

3D-point-based pipelines. Different from 2D images and 3D voxels, 3D points can preserve the 3D geospatial information as well as the internal local structure. Many point-based pipelines have been designed to process original points directly and thus no data transformation is needed (see Fig. 12).

Janssens-Coron and Guilbert (2019) made an initial endeavor utilizing PointNet (Qi et al., 2017a) to classify the ground points. Jin et al. (2020) implemented the GF of ALS point clouds via a point-based FCN. Similarly, Zhang et al. (2020) proposed a GF method based on EdgeConv (Wang et al., 2019) and PointNet (Qi et al.,

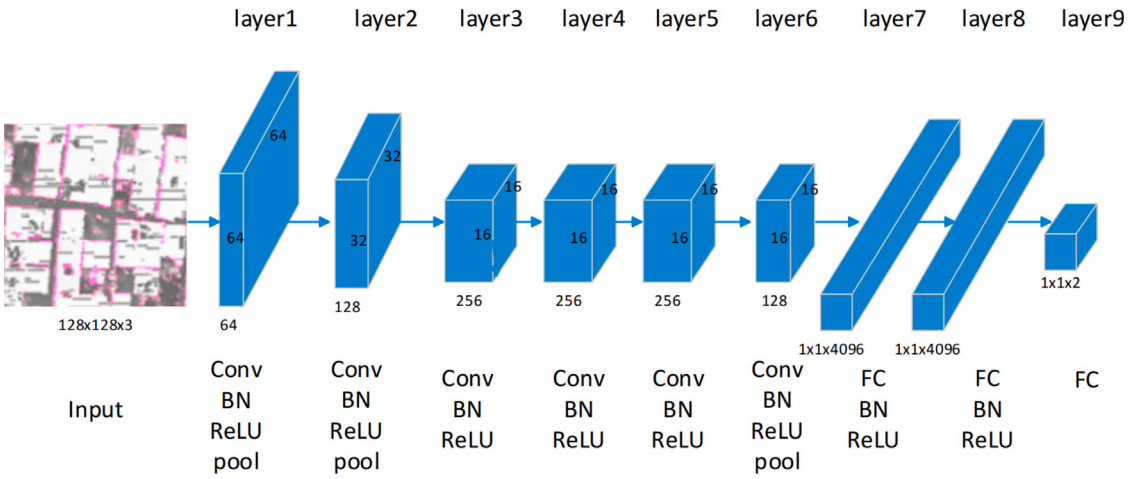

Fig. 10. An example of the 2D-image-based pipeline.
Source: Adapted from Hu and Yuan (2016), Fig. 3.

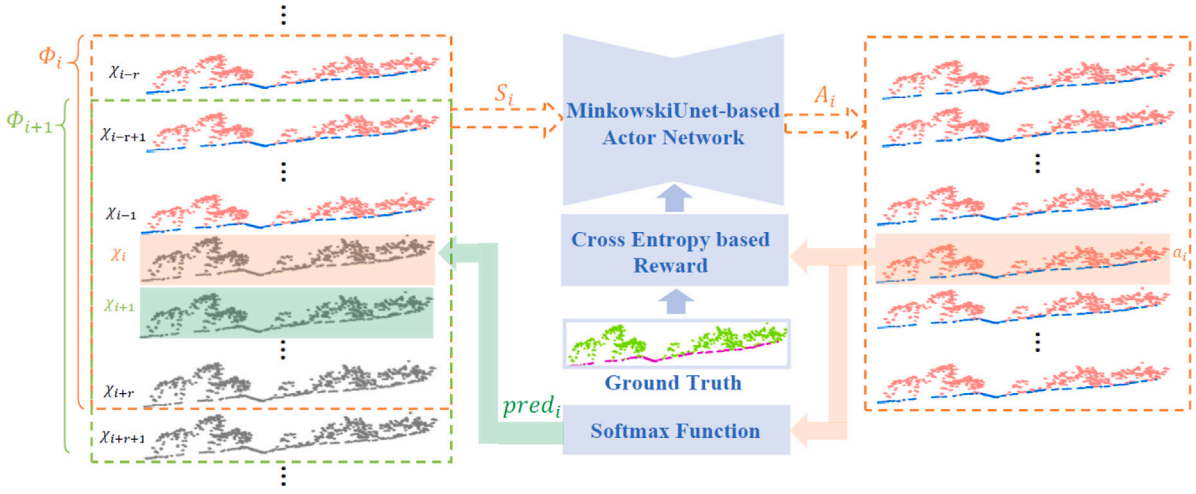

Fig. 11. An example of the 3D-voxel-based pipeline.
Source: Adapted from Dai et al. (2023), Fig. 4.

2017a). Krisanski et al. (2021) proposed a method based on improved PointNet++ (Qi et al., 2017b) to classify point clouds and extract DTMs. KPConv (Thomas et al., 2019), RandLA-Net (Hu et al., 2020) and SCF-Net (Fan et al., 2021) were also adapted for the GF of ALS Point clouds by Qin et al. (2021, 2023). In addition, Li et al. (2022) enhanced the KPConv (Thomas et al., 2019) with a self-attention mechanism to filter the ground from UAV-LS point clouds. Fareed et al. (2023) utilized PointCNN (Li et al., 2018) to implement the GF of UAV-LS point clouds in agricultural fields. To mitigate the reliance on extensive training samples, Nurunnabi et al. (2021) proposed a feature-based DL framework for GF.

The DL-based pipelines can achieve high classification accuracy in complex terrains, but they rely on a large number of training samples and may obtain unsatisfying results in challenging local areas (Qin et al., 2023).

In addition, there are also a number of DTM extraction methods highly relevant to the GF task (Lohmann, 2002; Jacobsen and Lohmann, 2003; Brovelli et al., 2004; Silván-Cárdenas and Wang, 2006; Chen et al., 2012a,b; Perko et al., 2015; Chen et al., 2016b; Mousa et al., 2017; Zhang et al., 2017; Gevaert et al., 2018; Mousa et al., 2019; Duan et al., 2019; Hingee et al., 2019; Luo et al., 2017; Amini Amirkolaee et al., 2022; Lê et al., 2022).

4. Available open-source tools for GF

In addition to being integrated into commercial software (e.g., TerraScan,[4] Agisoft Metashape,[5] ENVI LiDAR,[6] and Global Mapper LiDAR[7]), many of the aforementioned methods have been implemented in open-source tools (see Tables 4 and 5). Thanks to these selfless efforts, researchers can have a higher starting point to promote the development of novel GF methods. A brief description of the available open-source GF resources is provided below.

4.1. Free software with ground filters

ALDPAT[8] is an open-source LiDAR data processing software developed by the National Center for Airborne Laser Mapping. It integrates three different GF algorithms: the Maximum Local Slope Filtering

[4] https://terrasolid.com/products/terrascan/
[5] https://www.agisoft.com/
[6] https://www.l3harrisgeospatial.com/Software-Technology/ENVI/
[7] https://www.bluemarblegeo.com/global-mapper/
[8] http://LiDAR.ihrc.fiu.edu/LiDARtool.html

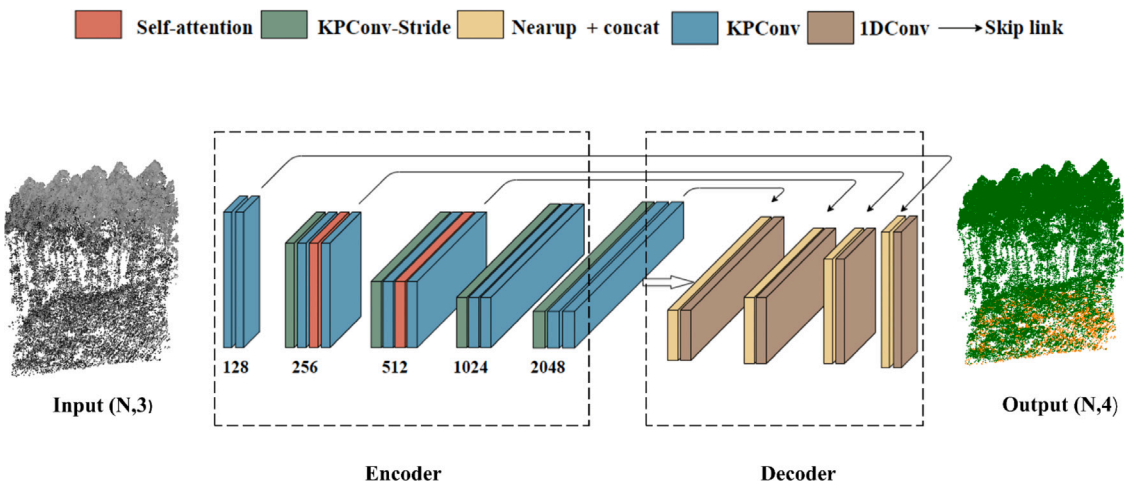

Fig. 12. An example of the 3D-point-based pipeline.
Source: Adapted from Li et al. (2022), Fig. 2.

Table 4
Free software with ground filters.

Software	Intergrated GF method	Method developer
ALDPAT[8]	MLSF; PMF; ETEWF	Vosselman (2000); Zhang et al. (2003); Zhang and Whitman (2005)
PCL[9]	PMF	Zhang et al. (2003)
PDAL[10]	PMF; SMRF; CSF	Zhang et al. (2003); Pingel et al. (2013); Zhang et al. (2016)
FUSION/LDV[11]	Linear-prediction-based	Kraus and Pfeifer (1998)
MCC-LiDAR[12]	MCC	Evans and Hudak (2007)
BCAL LiDAR Tools[13]	Interpolation-based	Streutker and Glenn (2006)
LASTools[14]	PTD	Axelsson (2000)
CloudCompare[15]	CSF	Zhang et al. (2016)

Table 5
Public DL models adapted for GF.

DL-based GF pipeline	Adapted DL model	Model developer
Hu and Yuan (2016)	VGG	Simonyan and Zisserman (2015)
Rizaldy et al. (2018)	FCN	Shelhamer et al. (2017)
Jin et al. (2020)	PointNet	Qi et al. (2017a)
Zhang et al. (2020)	PointNet; DGCNN	Qi et al. (2017a); Wang et al. (2019)
Qin et al. (2021)	PointNet++; KPConv; RandLA-Net	Qi et al. (2017b); Thomas et al. (2019); Hu et al. (2020)
Li et al. (2022)	KPConv	Thomas et al. (2019)
Dai et al. (2023)	MinkUNet; SCF-Net	Choy et al. (2019); Fan et al. (2021)

(MLSF) method (Vosselman, 2000), the PMF method (Zhang et al., 2003), and the Elevation Threshold with Extended Window Filtering (ETEWF) method (Zhang and Whitman, 2005).

PCL[9] is a popular open-source library for processing point cloud data. Real-time laser scanner processing, robotic and computer vision, and algorithm creation are the main areas of interest for the PCL library's developer community. It offers a C++ implementation of the PMF method (Zhang et al., 2003).

PDAL[10] is an open-source library that provides a series of LiDAR data processing capabilities, including GF. It offers the C++ implementations of the PMF (Zhang et al., 2003), SMRF (Pingel et al., 2013) and CSF (Zhang et al., 2016) methods.

FUSION/LDV[11] is an open-source LiDAR processing software with a primary intended use of forest stand analysis. Its "GroundFilter.exe" tool creates a bare-earth surface using the linear-prediction-based filter (Kraus and Pfeifer, 1998).

MCC-LiDAR[12] is an open-source programming application used to process point clouds in forested areas. The application can classify points as ground or non-ground with the MCC algorithm (Evans and Hudak, 2007).

BCAL LiDAR Tools[13] is a set of open-source software tools developed by the Bioinformatics and Computational Analytics Lab at the University of Maryland. These tools are designed for processing, analyzing and visualizing LiDAR data. The "Perform Height Filtering" tool can filter vegetation from the LiDAR data.

LASTools[14] is a collection of command-line tools for LiDAR data processing. It offers open-access tools and commercial tools. The open-access tools are available for reading and writing LAS/LAZ files.

[9] https://pointclouds.org/downloads/
[10] https://pdal.io
[11] http://forsys.sefs.uw.edu/fusion/fusionlatest.html
[12] http://sourceforge.net/projects/mccLiDAR/develop
[13] http://bcal.boisestate.edu/tools/LiDAR/
[14] http://www.cs.unc.edu/~isenburg/lastools/

Commercial licensing is necessary for more advanced interpolation, categorization, and filtering algorithms. The "lasground.exe" tool is a closed-source tool for ground extraction, which is based on the PTD algorithm (Axelsson, 2000).

CloudCompare[15] is a popular open-source software that provides a wide range of LiDAR processing capabilities. It can handle massive point clouds and has integrated the CSF algorithm (Zhang et al., 2016) as a plugin for GF.

4.2. Public DL models adapted for GF

VGG (Simonyan and Zisserman, 2015) is an early famous deep CNN model. The primary distinction between VGG and its forerunners is replacing convolutional layers with large receptive fields with ones with small receptive fields to form a deeper network.

FCN (Shelhamer et al., 2017) is regarded as a milestone work for semantic segmentation. DCNNs are utilized in this model as powerful visual models capable of learning feature hierarchies. This model effectively showcases how CNNs can be used for semantic segmentation tasks, regardless of the input size.

PointNet/PointNet++ (Qi et al., 2017a,b) is the first investigation into point-based DL architectures that directly process points with multi-layer perceptrons. To surmount the constraint of local receptive fields in PointNet, geometrical features are hierarchically extracted at different scales in the PointNet++ pipeline.

MinkUNet (Choy et al., 2019) is a 3D DNN with sparse convolutions as the core operation. It exploits the intrinsic sparsity of point clouds and makes 3D CNN architectures applicable for large-scale point cloud processing.

DGCNN (Wang et al., 2019) is a 3D DNN featuring edge convolution. In order to fully explore local and global information, dynamic graphs are used for feature aggregation in this model.

KPConv (Thomas et al., 2019) is a 3D DNN utilizing kernel point convolution as convolutional operations. It is implemented in continuous domains. The linear correlation between the positions of the points and the kernel points defines the weights of the points assigned to different regions within the convolutional kernels. The learnability of the kernel point positions allows the convolutional kernels to conform more effectively to local structures.

RandLA-Net (Hu et al., 2020) is a 3D DNN that aims to facilitate the efficient interpretation of point clouds on a large scale. It is based on random sampling. Several modules for aggregating local features are made to obtain intricate local geometry. The feature aggregators carefully pool the encoded features to the center point after first using MLPs to encode relative point locations in nearby neighborhoods.

SCF-Net (Fan et al., 2021) is a 3D DNN which can effectively learn spatial contextual features from large-scale point clouds. SCF-Net attained the foremost level of performance on multiple point cloud benchmarks.

5. Summary of evaluations on public benchmark datasets

To date, many comparative studies of GF methods have been conducted, but most of them focus on comparisons of traditional GF algorithms on relatively small or specific study sites (Sithole and Vosselman, 2004; Baligh et al., 2008; Korzeniowska et al., 2014; Luis Montealegre et al., 2015; Stereńczak et al., 2016; Zhao et al., 2018; Silva et al., 2018; Serifoglu Yilmaz et al., 2018; Serifoglu Yilmaz and Gungor, 2018; Klápště et al., 2020; Moudry et al., 2020; Chen et al., 2021). Recently, the newly proposed OpenGF dataset provides a good opportunity for evaluating the performance of advanced DL techniques in GF. This section aims to conduct systematic comparative analyses of experimental results on current public GF benchmark datasets, where all results are extracted from the corresponding publications. The implementation details of the compared methods can be obtained from the corresponding original papers.

[15] https://www.cloudcompare.org

5.1. Evaluations on OpenGF

The initial baselines of the OpenGF benchmark (Qin et al., 2021) include two traditional GF methods and three 3D DNNs. Recently, the benchmark has been further updated with more new test data and methods (Qin et al., 2023; Dai et al., 2023). Fig. 13 displays the GF results of several representative approaches on the test set of OpenGF.

From the existing evaluations, some inferences could be drawn as follows: (1) 3D DNNs consistently have better performance than traditional GF methods in hybrid terrain scenes, as evidenced by the superior OA and $RMSE$. In addition, traditional GF methods are prone to significant fluctuations when applied to different topography regions, while 3D DNNs exhibit greater performance adaptability in hybrid landforms. (2) 3D DNNs are less affected by outliers compared to traditional GF methods, perhaps because traditional GF methods tend to assume the lowest local points being the ground, whereas 3D DNNs do not make such assumptions during point classification. (3) 3D DNNs demonstrate higher classification accuracy compared to traditional GF methods in complex mountain terrains, despite both kinds of methods exhibiting unsatisfactory performance in terms of $RMSE$.

5.2. Evaluations on ISPRS-Filtertest

The performance of eight traditional GF methods was initially compared by Sithole and Vosselman (2004) on the ISPRS-Filtertest dataset to identify future research directions in the field of GF. The comparative experiments show that all tested GF methods demonstrate effective performance in areas with relatively even topography but tend to make misclassifications in complex urban scenes and disconnected terrains. Inspired by this research, many new GF approaches have been designed and tested on the ISPRS-Filtertest dataset. Fig. 14 shows the average OAs achieved by a series of representative methods on ISPRS-Filtertest. Note that, due to lacking sufficient samples for training, the performance of 3D DNNs on ISPRS-Filtertest is obtained by testing their models that trained on OpenGF (Qin et al., 2023).

According to Figs. 14 and 13, some observations could be listed as follows: (1) Many traditional GF methods achieved better average OA than the trained DL models. (2) Compared to their performance on the OpenGF dataset, the trained DL models performed relatively poorly on the ISPRS-Filtertest dataset. This can be attributed to domain gaps between different datasets. (3) There exists an obvious difference in cross-dataset generalization performance between different DL models.

6. Challenges and directions

6.1. Remaining challenges

Over the past few decades, considerable endeavors have been undertaken to enhance the performance of conventional ground filters. For instance, researchers have explored various approaches such as incorporating supplementary information (Kim et al., 2013; Debella-Gilo, 2016), landscape decomposition (Qin et al., 2018), and automatic parameter tuning (Shi et al., 2018; Liu et al., 2020). Yet, there is still a significant gap between the state-of-the-art results and human-level performance in practice. Furthermore, the application of advanced DL techniques to GF presents novel challenges. Overall, there are two common problems faced by existing GF techniques to solve:

(1) **Unstable filtering performance**. Unsupervised ground filters are difficult to apply to hybrid scenes, due to their performance relies heavily on appropriate parameter settings. While supervised learning-based methods are highly adaptive to different scenes, they tend to overfit the domain distribution of the training data, resulting in degrading performance on new data with different distributions.

(2) **Unsatisfied micro-terrain errors**. In complex scenes, traditional ground filters commonly encounter difficulties in preserving

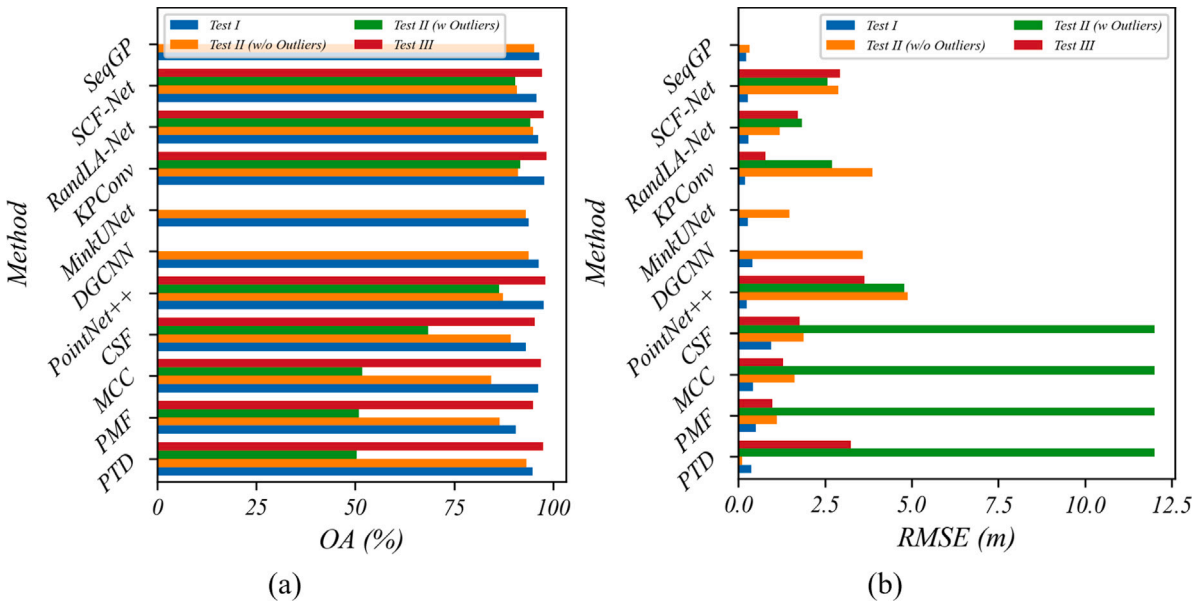

Fig. 13. The *OA*s (a) and *RMSE*s (b) achieved by different methods on the test set of OpenGF. Note that, the results achieved by DGCNN, MinkUnet and SeqGP come from Dai et al. (2023), and the remaining results come from Qin et al. (2023). Since MinkUnet, DGCNN, and SeqGP were not tested on Test II (w outliers) and Test III, the relevant results are missing. In addition, the *RMSE*s achieved by traditional GF methods on Test II (w outliers) are very large and are not fully displayed.

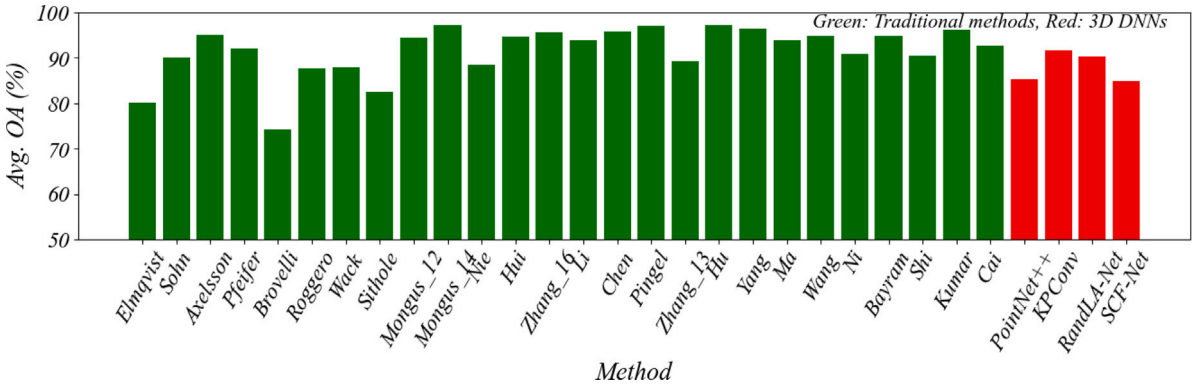

Fig. 14. The average *OA*s achieved by different methods on ISPRS-Filtertest. Note that, the *OA*s of traditional GF methods (Elmqvist et al., 2001; Sohn and Dowman, 2002; Axelsson, 2000; Pfeifer et al., 2001; Brovelli et al., 2002; Roggero, 2001; Wack and Wimmer, 2002; Sithole, 2001; Mongus and Žalik, 2012; Mongus et al., 2014; Nie et al., 2017; Hui et al., 2016; Zhang et al., 2016; Li et al., 2017; Chen et al., 2013; Pingel et al., 2013; Zhang and Lin, 2013; Hu et al., 2014; Yang et al., 2016; Ma and Li, 2019; Wang et al., 2017; Ni et al., 2018; Bayram et al., 2018; Shi et al., 2018; Kumar et al., 2018; Cai et al., 2019) are converted from the equivalent *Total* errors.

crucial ground points or removing low object points within local challenging areas. Although learning-based methods can achieve better performance in these areas, they may make incomprehensible misclassifications in relatively simple areas. In particular, supervised learning-based methods cannot provide a self-explainable theory for these silly mistakes.

6.2. Future directions

Firstly, regarding the challenge of **"Unstable filtering performance"**, cross-fertilization among computer vision, computer graphics, and control theory would be a necessary approach to enable fast improvement. Specifically, two directions are listed below:

(1) **Physical engine for sample generation.** The most direct way of improving the performance of supervised learning is to increase the number of training data. However, the situation in practice is much more complex than that considered in existing public datasets. Although current public 3D geospatial datasets provide lots of high-quality labeled samples from different scenes, they still cannot fully meet the needs of practical applications. Since data collection and manual annotation often require expensive costs, several works have begun to explore how to directly synthesize annotated 3D datasets. In particular, recent works have begun to study the synthesis of outdoor 3D point clouds using physical engines (Gaidon et al., 2016; Ros et al., 2016; Yue et al., 2018; Chen et al., 2022). In addition, the rapidly developing Artificial Intelligence Generated Content (AIGC) techniques also provide a promising possibility for 3D sample generation (Wang et al., 2023).

(2) **Self-supervised/unsupervised learning.** Developing self-supervised or unsupervised learning techniques is another way to mitigate the problem of limited model generalization due to insufficient training data. Recently, a handful of works have tried to train networks on a large amount of unlabeled point clouds using self-supervised/unsupervised learning techniques. These pre-trained models have been demonstrated more effective for a series of downstream tasks (Xie et al., 2020; Zhang et al., 2021; Wang et al., 2021; Liu et al., 2022).

Secondly, the key point for solving the problem of **"Unsatisfied micro-terrain errors"** is to build a hybrid framework combining the existing DL pipelines with physical criteria. Specifically, this problem can be alleviated from the following two aspects:

(1) **Incorporating domain knowledge into DL**. The internal working mechanisms of DL models are still unclear, which raises the important question of whether the DL model can perform as expected under various conditions (Ribeiro et al., 2016). Incorporating physics laws into supervised-learning-based approaches is a promising way to improve the interpretability of data-driven models. e.g., Embedding physical rules by adding physical-based terms into the loss function.

(2) **Replacing simple rules with DL**. An alternative solution is the partial use of DL models within traditional frameworks to improve computational efficiency and performance accuracy. For example, due to the limitations of the artificial rules used, the traditional PTD method is easy to lose many steep ground points, which leads to algorithm failure in mountain areas. If the learning-based ground classification model is embedded into the ground point discrimination step of PTD, the performance of PTD in mountain areas may be improved.

6.3. Beyond GF: Implications for large-scale 3D geospatial understanding

Early aerial photogrammetric point clouds and ALS point clouds were relatively sparse, resulting in less demand for accurate object-level semantic labeling. Therefore, early research mainly focused on ground extraction, or large object detection (e.g., roofs). With the development of dense point cloud acquisition technology (e.g., UAV LiDAR and advanced dense image matching techniques) and the deepening of natural resource investigation, smart city, autonomous driving, meta-universe and other applications, the demand for large-scale 3D geospatial understanding is becoming increasingly prominent, especially in urban areas. Although this study focuses on the GF task, it provides some important implications for high-level semantic interpretations of large-scale outdoor 3D point clouds as follows:

(1) **Reasoning recognition is important**. In practice, most of the errors in the automatic filtering results are visually unintuitive and difficult to distinguish. To eliminate these errors, according to the common sense that it is impossible to have two or more ground points with different elevations in the same plane position, the staff usually extracts a series of profiles from points and infers possible misclassified ground points which do not have a smooth elevation transition with surrounding ground points. This manual refinement operation implies that reasoning recognition is important for large-scale 3D geospatial understanding. How to model human reasoning and recognition behaviors as a computational theory and method (Akula et al., 2022) will be a scientific research direction worthy of careful study.

(2) **Joint formulation is encouraged**. As demonstrated in the experiments presented in Section 5.2, the performance of state-of-the-art DL models in the low-level GF task across different datasets is unstable. This indicates that the problem of the limited generalization ability of the existing DL models in high-level 3D geospatial understanding tasks will be more serious. Developing a tractable framework to link the GF task with the semantic segmentation task will bring together the earth observation and computer vision communities, potentially could provide a much better semantic understanding of ALS point clouds. It is valuable to incorporate GF into the semantic segmentation workflow, and redefine it as the post-refinement of the ground classification result.

7. Summary

This paper provides a comprehensive survey of up-to-date GF studies, aiming to promote the research of more intelligent techniques for GF. Firstly, a comprehensive review of up-to-date and advanced GF methods was presented. Secondly, systematic comparisons of existing experimental results on public GF benchmark datasets were conducted. Additionally, this survey collected the latest public resources that can be exploited for the GF research, including relevant datasets and metrics, as well as a series of open-source tools. Finally, the remaining challenges and promising directions in the GF research, along with implications for large-scale 3D geospatial understanding, were summarized and discussed.

Through extensive investigation, it can be concluded that: (1) The earth's surface is extremely complex and diverse, which makes it difficult to establish a unified theory and method to completely solve the GF problem. (2) The attainment of truly intelligent GF still requires a lot of fundamental research, especially in complex environments. (3) It is imperative to develop advanced techniques tailored to GF, since simply applying advanced theories and technologies in relevant fields may not solve the GF problem perfectly.

Furthermore, the remaining challenges in the GF task mainly lie in unstable filtering performance and unsatisfied micro-terrain errors. In response to these issues, future GF research directions include two main aspects: (1) Cross-fertilization among computer vision, computer graphics, and control theory. (2) Hybrid framework to combine the DL with physical criteria.

Finally, joint formulations of the GF and 3D semantic segmentation tasks are encouraged to better support a series of emerging downstream applications.

Declaration of competing interest

The authors declare that they have no known competing financial interests or personal relationships that could have appeared to influence the work reported in this paper.

Data availability

No data was used for the research described in the article.

Acknowledgments

This work was partially supported by the National Natural Science Foundation of China [grant numbers 42001400, 42101451] and the Startup Foundation for Introducing Talent of Nanjing University of Information Science and Technology, China [grant number 2023r093].

References

Abdeldayem, Z., 2019. Automatic weighted splines filter (AWSF): A new algorithm for extracting terrain measurements from raw LiDAR point clouds. IEEE J. Sel. Top. Appl. Earth Obs. Remote Sens. 13, 60–71.

Akula, A.R., Wang, K., Liu, C., Saba-Sadiya, S., Lu, H., Todorovic, S., Chai, J., Zhu, S.C., 2022. CX-ToM: Counterfactual explanations with theory-of-mind for enhancing human trust in image recognition models. iScience 25 (1), 103581.

Amini Amirkolaee, H., Arefi, H., Ahmadlou, M., Raikwar, V., 2022. DTM extraction from DSM using a multi-scale DTM fusion strategy based on deep learning. Remote Sens. Environ. 274, 113014.

Andersen, H.E., Reutebuch, S.E., McGaughey, R.J., d'Oliveira, M.V., Keller, M., 2014. Monitoring selective logging in western Amazonia with repeat lidar flights. Remote Sens. Environ. 151, 157–165.

Arefi, H., Hahn, M., 2005. A morphological reconstruction algorithm for separating off-terrain points from terrain points in laser scanning data. In: ISPRS WG III/3, III/4, V/3 Workshop "Laserscanning 2005". pp. 120–125.

Axelsson, P., 2000. DEM generation from laser scanner data using adaptive TIN models. Int. Arch. Photogramm. Remote Sens. XXXIII, Part B4, 110–117.

Ayazi, S.M., Saadat Seresht, M., 2019. Comparison of traditional and machine learning base methods for ground point cloud labeling. Int. Arch. Photogramm. Remote Sens. Spatial Inf. Sci. XLII-4/W18, 141–145.

Baligh, A., Zoej, M.V., Mohammadzadeh, A., 2008. Bare earth extraction from airborne LiDAR data using different filtering methods. Int. Arch. Photogramm. Remote Sens. Spatial Inf. Sci. XXXVII, 237–240.

Bao, Y., Li, G., Cao, C., Li, X., Zhang, H., He, Q., Bai, L., Chang, C., 2008. Classification of Lidar point cloud and generation of DTM from LiDAR height and intensity data in forested area. Int. Arch. Photogramm. Remote Sens. Spatial Inf. Sci. XXXVII, 313–318.

Bartels, M., Wei, H., 2006a. Segmentation of LIDAR data using measures of distribution. Int. Arch. Photogramm. Remote Sens. Spatial Inf. Sci. 36 (7), 426–431.

Bartels, M., Wei, H., 2006b. Towards DTM generation from LiDAR data in hilly terrain using wavelets. In: Proceedings of 4th International Workshop on Pattern Recognition in Remote Sensing in Conjunction with ICPR 2006. pp. 33–36.

Bartels, M., Wei, H., 2010. Threshold-free object and ground point separation in LIDAR data. Pattern Recognit. Lett. 31 (10), 1089–1099.

Bayram, E., Frossard, P., Vural, E., Alatan, A., 2018. Analysis of airborne LiDAR point clouds with spectral graph filtering. IEEE Geosci. Remote Sens. Lett. 15 (8), 1284–1288.

Behley, J., Garbade, M., Milioto, A., Quenzel, J., Behnke, S., Stachniss, C., Gall, J., 2019. SemanticKITTI: A dataset for semantic scene understanding of LiDAR sequences. In: Proc. IEEE Int. Conf. Comput. Vis.. pp. 9296–9306.

Brovelli, M., Cannata, M., Longoni, U., 2002. Managing and processing LIDAR data within GRASS. In: Proceedings of the Open Source GIS-GRASS Users Conference 2002. https://citeseerx.ist.psu.edu/viewdoc/summary?doi=10.1.1.19.8294. (Accessed 7 November 2023).

Brovelli, M.A., Cannata, M., Longoni, U.M., 2004. LIDAR data filtering and DTM interpolation within GRASS. Trans. GIS 8, 155–174.

Bulatov, D., Stütz, D., Hacker, J., Weinmann, M., 2021. Classification of airborne 3D point clouds regarding separation of vegetation in complex environments. Appl. Opt. 60 (22), F6–F20.

Cai, S., Zhang, W., Liang, X., Wan, P., Qi, J., Yu, S., Yan, G., Shao, J., 2019. Filtering airborne LiDAR data through complementary cloth simulation and progressive TIN densification filters. Remote Sens. 11 (9), 1037.

Canuto, M.A., Estrada-Belli, F., Garrison, T.G., Houston, S.D., Acuña, M.J., Kováč, M., Marken, D., Nondédéo, P., Auld-Thomas, L., Castanet, C., et al., 2018. Ancient lowland Maya complexity as revealed by airborne laser scanning of northern Guatemala. Science 361 (6409), eaau0137.

Che, E., Senogles, A., Olsen, M.J., 2021. Vo-smog: A versatile, smooth segment-based ground filter for point clouds via multi-scale voxelization. ISPRS Ann. Photogramm. Remote Sens. Spatial Inf. Sci. VIII-4/W2-2021, 59–66.

Chen, H., Cheng, M., Li, J., Liu, Y., 2012a. An iterative terrain recovery approach to automated DTM generation from airborne LiDAR point clouds. Int. Arch. Photogrammetry, Remote Sens. Spatial Inf. Sci. XXXIX-B4, 363–368.

Chen, Z., Devereux, B., Gao, B., Amable, G., 2012b. Upward-fusion urban DTM generating method using airborne Lidar data. ISPRS J. Photogramm. Remote Sens. 72, 121–130.

Chen, Z., Gao, B., Devereux, B., 2017. State-of-the-art: DTM generation using airborne LIDAR data. Sensors 17 (1), 150.

Chen, Q., Gong, P., Baldocchi, D., Xie, G., 2007. Filtering airborne laser scanning data with morphological methods. Photogramm. Eng. Remote Sens. 73 (2), 175–185.

Chen, C., Guo, J., Wu, H., Li, Y., Shi, B., 2021. Performance comparison of filtering algorithms for high-density airborne LiDAR point clouds over complex LandScapes. Remote Sens. 13 (14), 2663.

Chen, M., Hu, Q., Yu, Z., Thomas, H., Feng, A., Hou, Y., McCullough, K., Ren, F., Soibelman, L., 2022. STPLS3D: A large-scale synthetic and real aerial photogrammetry 3D point cloud dataset. In: Proc. British Machine Vis. Conf. https://bmvc2022.mpi-inf.mpg.de/0429.pdf. (Accessed 7 November 2023).

Chen, C., Li, Y., Li, W., Dai, H., 2013. A multiresolution hierarchical classification algorithm for filtering airborne LiDAR data. ISPRS J. Photogramm. Remote Sens. 82, 1–9.

Chen, Q., Wang, H., Zhang, H., Sun, M., Liu, X., 2016a. A point cloud filtering approach to generating DTMs for steep mountainous areas and adjacent residential areas. Remote Sens. 8 (1), 71.

Chen, Z., Xu, B., Gao, B., 2016b. An image-segmentation-based urban DTM generation method using airborne Lidar data. IEEE J. Sel. Top. Appl. Earth Obs. Remote Sens. 9 (1), 496–506.

Choy, C., Gwak, J., Savarese, S., 2019. 4D spatio-temporal ConvNets: Minkowski convolutional neural networks. In: Proc. IEEE Conf. Comput. Vis. Pattern Recog. pp. 3075–3084.

Crosilla, F., Visintini, D., Prearo, G., 2004. A robust method for filtering non-ground measurements from airborne LiDAR data. Int. Arch. Photogramm. Remote Sens. Spatial Inf. Sci. 2004, 196–201.

Dai, H., Hu, X., Shu, Z., Qin, N., Zhang, J., 2023. Deep ground filtering of large-scale ALS point clouds via iterative sequential ground prediction. Remote Sens. 15 (4), 961.

Debella-Gilo, M., 2016. Bare-earth extraction and DTM generation from photogrammetric point clouds including the use of an existing lower-resolution DTM. Int. J. Remote Sens. 37 (13), 3104–3124.

Doneus, M., Mandlburger, G., Doneus, N., 2020. Archaeological ground point filtering of airborne laser scan derived point-clouds in a difficult mediterranean environment. J. Comput. Appl. Archaeol. 3 (1), 92–108.

Dong, Y., Cui, X., Zhang, L., Ai, H., 2018. An improved progressive TIN densification filtering method considering the density and standard variance of point clouds. ISPRS Int. J. Geo-Inf. 7 (10), 409.

Duan, L., Desbrun, M., Giraud, A., Trastour, F., Laurore, L., 2019. Large-scale DTM generation from satellite data. In: Proc. IEEE Conf. Comput. Vis. Pattern Recog. Workshops. pp. 1442–1450.

Elmqvist, M., 2002. Ground surface estimation from airborne laser scanner data using active shape models. Int. Arch. Photogramm. Remote Sens. XXXIV, 114–118.

Elmqvist, M., Jungert, E., Lantz, F., Persson, A., Soderman, U., 2001. Terrain modelling and analysis using laser scanner data. Int. Arch. Photogramm. Remote Sens. XXXIV-3/W4, 219–226.

Evans, J.S., Hudak, A.T., 2007. A multiscale curvature algorithm for classifying discrete return LiDAR in forested environments. IEEE Trans. Geosci. Remote Sens. 45 (4), 1029–1038.

Fan, S., Dong, Q., Zhu, F., Lv, Y., Ye, P., Wang, F.-Y., 2021. SCF-Net: Learning spatial contextual features for large-scale point cloud segmentation. In: Proc. IEEE Conf. Comput. Vis. Pattern Recog.. pp. 14504–14513.

Fareed, N., Flores, J.P., Das, A.K., 2023. Analysis of UAS-LiDAR ground points classification in agricultural fields using traditional algorithms and PointCNN. Remote Sens. 15 (2), 483.

Gaidon, A., Wang, Q., Cabon, Y., Vig, E., 2016. Virtual worlds as proxy for multi-object tracking analysis. In: Proc. IEEE Conf. Comput. Vis. Pattern Recog. pp. 4340–4349.

Geiger, A., Lenz, P., Urtasun, R., 2012. Are we ready for autonomous driving? The KITTI vision benchmark suite. In: Proc. IEEE Conf. Comput. Vis. Pattern Recog. pp. 3354–3361.

Gevaert, C., Persello, C., Nex, F., Vosselman, G., 2018. A deep learning approach to DTM extraction from imagery using rule-based training labels. ISPRS J. Photogramm. Remote Sens. 142, 106–123.

Gomes, T., Matias, D., Campos, A., Cunha, L., Roriz, R., 2023. A survey on ground segmentation methods for automotive LiDAR sensors. Sensors 23 (2), 601.

Guan, H., Li, J., Yu, Y., Zhong, L., Ji, Z., 2014. DEM generation from lidar data in wooded mountain areas by cross-section-plane analysis. Int. J. Remote Sens. 35, 927–948.

Hackel, T., Savinov, N., Ladicky, L., Wegner, J.D., Schindler, K., Pollefeys, M., 2017. Semantic3D.net: A new large-scale point cloud classification benchmark. ISPRS Ann. Photogramm. Remote Sens. Spatial Inf. Sci. IV-1-W1, 91–98.

He, Y., Zhang, C., Fraser, C.S., 2018. Progressive filtering of airborne LiDAR point clouds using graph cuts. IEEE J. Sel. Top. Appl. Earth Obs. Remote Sens. 11 (8), 2933–2944.

Hingee, K.L., Caccetta, P., Caccetta, L., 2019. Modelling discontinuous terrain from DSMs using segment labelling, outlier removal and thin-plate splines. ISPRS J. Photogramm. Remote Sens. 155, 159–171.

Hou, W., Wang, X., Zhang, C., Ji, Z., Zhang, X., 2014. Minimum spanning tree-based digital terrain model detection from light detection and ranging points. Inverse Probl. Sci. Eng. 22 (6), 988–1001.

Hu, H., Ding, Y., Zhu, Q., Wu, B., Lin, H., Du, Z., Zhang, Y., Zhang, Y., 2014. An adaptive surface filter for airborne laser scanning point clouds by means of regularization and bending energy. ISPRS J. Photogramm. Remote Sens. 92, 98–111.

Hu, Q., Yang, B., Khalid, S., Xiao, W., Trigoni, N., Markham, A., 2022. SensatUrban: Learning semantics from urban-scale photogrammetric point clouds. Int. J. Comput. Vis. 130, 316–343.

Hu, Q., Yang, B., Xie, L., Rosa, S., Guo, Y., Wang, Z., Trigoni, N., Markham, A., 2020. RandLA-Net: Efficient semantic segmentation of large-scale point clouds. In: Proc. IEEE Conf. Comput. Vis. Pattern Recog.. pp. 11105–11114.

Hu, X., Ye, L., Pang, S., Shan, J., 2015. Semi-global filtering of airborne LiDAR data for fast extraction of digital terrain models. Remote Sens. 7 (8), 10996–11015.

Hu, X., Yuan, Y., 2016. Deep-learning-based classification for DTM extraction from ALS point cloud. Remote sens. 8 (9), 730.

Hui, Z., Hu, Y., Yevenyo, Y.Z., Yu, X., 2016. An improved morphological algorithm for filtering airborne LiDAR point cloud based on multi-level kriging interpolation. Remote Sens. 8 (1), 35.

Hui, Z., Jin, S., Xia, Y., Nie, Y., Xie, X., Li, N., 2021. A mean shift segmentation morphological filter for airborne LiDAR DTM extraction under forest canopy. Opt. Laser Technol. 136, 106728.

Hui, Z., Li, D., Jin, S., Ziggah, Y.Y., Wang, L., Hu, Y., 2019. Automatic DTM extraction from airborne LiDAR based on expectation-maximization. Opt. Laser Technol. 112, 43–55.

Jacobsen, K., Lohmann, P., 2003. Segmented filtering of laser scanner DSMs. Int. Arch. Photogramm. Remote Sens. Spat. Inf. Sci. XXXIV-3/W13, https://www.isprs.org/proceedings/XXXIV/3-W13/papers/Jacobsen_ALSDD2003.pdf. (Accessed 7 November 2023).

Jahromi, A.B., Zoej, M.J.V., Mohammadzadeh, A., Sadeghian, S., 2011. A novel filtering algorithm for bare-earth extraction from airborne laser scanning data using an artificial neural network. IEEE J. Sel. Top. Appl. Earth Obs. Remote Sens. 4 (4), 836–843.

Jakovljevic, G., Govedarica, M., Alvarez-Taboada, F., Pajic, V., 2019. Accuracy assessment of deep learning based classification of LiDAR and UAV points clouds for DTM creation and flood risk mapping. Geosciences 9 (7), 323.

Janssens-Coron, E., Guilbert, E., 2019. Ground point filtering from airborne LIDAR point clouds using deep learning: A preliminary study. Int. Arch. Photogramm. Remote Sens. Spatial Inf. Sci. XLII-2/W13, 1559–1565.

Jin, S., Su, Y., Zhao, X., Hu, T., Guo, Q., 2020. A point-based fully convolutional neural network for airborne LiDAR ground point filtering in forested environments. IEEE J. Sel. Top. Appl. Earth Obs. Remote Sens. 13, 3958–3974.

Kilian, J., Haala, N., Englich, M., Iii, C., 1996. Capture and evaluation of airborne laser scanner data. Int. Arch. Photogramm. Remote Sens. XXXI, 383–388.

Kim, Y.M., Eo, Y.D., Chang, A.J., Kim, Y.I., 2013. Generation of a DTM and building detection based on an MPF through integrating airborne lidar data and aerial images. Int. J. Remote Sens. 34 (8), 2947–2968.

Klápště, P., Fogl, M., Barták, V., Gdulová, K., Urban, R., Moudrý, V., 2020. Sensitivity analysis of parameters and contrasting performance of ground filtering algorithms with UAV photogrammetry-based and LiDAR point clouds. Int. J. Digit. Earth 13 (12), 1672–1694.

Kobler, A., Pfeifer, N., Ogrinc, P., Todorovski, L., Oštir, K., Džeroski, S., 2007. Repetitive interpolation: A robust algorithm for DTM generation from Aerial Laser Scanner Data in forested terrain. Remote Sens. Environ. 108 (1), 9–23.

Kölle, M., Laupheimer, D., Schmohl, S., Haala, N., Rottensteiner, F., Wegner, J.D., Ledoux, H., 2021. The hessigheim 3D (H3D) benchmark on semantic segmentation of high-resolution 3D point clouds and textured meshes from UAV LiDAR and multi-view-stereo. ISPRS Open J. Photogramm. Remote Sens. 1, 100001.

Korzeniowska, K., Pfeifer, N., Mandlburger, G., Lugmayr, A., 2014. Experimental evaluation of ALS point cloud ground extraction tools over different terrain slope and land-cover types. Int. J. Remote Sens. 35 (13), 4673–4697.

Kraus, K., Pfeifer, N., 1998. Determination of terrain models in wooded areas with airborne laser scanner data. ISPRS J. Photogramm. Remote Sens. 53 (4), 193–203.

Kraus, K., Pfeifer, N., 2001. Advanced DTM generation from LIDAR data. Int. Arch. Photogramm. Remote Sens. Spatial Inf. Sci. 34 (3/W4), 23–30.

Krisanski, S., Taskhiri, M.S., Gonzalez Aracil, S., Herries, D., Turner, P., 2021. Sensor agnostic semantic segmentation of structurally diverse and complex forest point clouds using deep learning. Remote Sens. 13 (8), 1413.

Kumar, B., Yadav, M., Lohani, B., Singh, A.K., 2018. A two-stage algorithm for ground filtering of airborne laser scanning data. Int. J. Remote Sens. 39 (20), 6757–6783.

Lê, H.A., Guiotte, F., Pham, M.T., Lefèvre, S., Corpetti, T., 2022. Learning digital terrain models from point clouds: ALS2DTM dataset and rasterization-based GAN. IEEE J. Sel. Top. Appl. Earth Obs. Remote Sens. 15, 4980–4989.

Lee, H., Younan, N., 2003. DTM extraction of lidar returns via adaptive processing. IEEE Trans. Geosci. Remote Sens. 41 (9), 2063–2069.

Li, Y., Bu, R., Sun, M., Wu, W., Di, X., Chen, B., 2018. PointCNN: Convolution on X-transformed points. In: Proc. Adv. Neural Inf. Process. Syst.. pp. 828–838.

Li, X., Li, C., Tong, Z., Lim, A., Yuan, J., Wu, Y., Tang, J., Huang, R., 2020. Campus3D: A photogrammetry point cloud benchmark for hierarchical understanding of outdoor scene. In: Proceedings of the 28th ACM International Conference on Multimedia. pp. 238–246.

Li, B., Lu, H., Wang, H., Qi, J., Yang, G., Pang, Y., Dong, H., Lian, Y., 2022. Terrain-Net: A highly-efficient, parameter-free, and easy-to-use deep neural network for ground filtering of UAV LiDAR data in forested environments. Remote Sens. 14 (22), 5798.

Li, S., Sun, H., Yan, L., 2011. A filtering method for generating DTM based on multi-scale mathematic morphology. In: 2011 IEEE International Conference on Mechatronics and Automation. pp. 693–697.

Li, Y., Yong, B., Van Oosterom, P., Lemmens, M., Wu, H., Ren, L., Zheng, M., Zhou, J., 2017. Airborne LiDAR data filtering based on geodesic transformations of mathematical morphology. Remote Sens. 9 (11), 1104.

Li, Y., Yong, B., Wu, H., An, R., Xu, H., 2014. An improved top-hat filter with sloped brim for extracting ground points from airborne lidar point clouds. Remote Sens. 6, 12885–12908.

Lin, X., Zhang, J., 2014. Segmentation-based filtering of airborne LiDAR point clouds by progressive densification of terrain segments. Remote Sens. 6 (2), 1294–1326.

Liu, X., 2008. Airborne LiDAR for DEM generation:Some critical issues. Prog. Phys. Geog. 32, 31–49.

Liu, H., Cai, M., Lee, Y.J., 2022. Masked discrimination for self-supervised learning on point clouds. In: Proc. Eur. Conf. Comput. Vis. pp. 657–675.

Liu, L., Lim, S., 2018. A voxel-based multiscale morphological airborne lidar filtering algorithm for digital elevation models for forest regions. Measurement 123, 135–144.

Liu, X., Zhang, Y., Huang, X., Wan, Y., Wang, S., 2020. Terrain-adaptive ground filtering of airborne LiDAR data based on saliency-aware thin plate spline. Int. Arch. Photogramm. Remote Sens. Spatial Inf. Sci. XLIII-B2-2020, 279–285.

Lohmann, P., 2002. Segmentation and filtering of laser scanner digital surface models. Int. Arch. Photogramm. Remote Sens. Spat. Inf. Sci. XXXIV, Part 2, 311–316.

Lohmann, P., Koch, A., Schaeffer, M., 2000. Approaches to the filtering of laser scanner data. Int. Arch. Photogramm. Remote Sens. XXXIII, Part B3, 540–547.

Lu, W.L., Murphy, K.P., Little, J.J., Sheffer, A., Fu, H., 2009. A hybrid conditional random field for estimating the underlying ground surface from airborne LiDAR data. IEEE Trans. Geosci. Remote Sens. 47 (8), 2913–2922.

Luis Montealegre, A., Teresa Lamelas, M., de la Riva, J., 2015. A comparison of open-source LiDAR filtering algorithms in a mediterranean forest environment. IEEE J. Sel. Top. Appl. Earth Obs. Remote Sens. 8 (8), 4072–4085.

Luo, Y., Ma, H., Zhou, L., 2017. DEM retrieval from airborne LiDAR point clouds in mountain areas via deep neural networks. IEEE Geosci. Remote Sens. Lett. 14 (10), 1770–1774.

Ma, W., Li, Q., 2019. An improved ball pivot algorithm-based ground filtering mechanism for LiDAR data. Remote Sens. 11 (10), 1179.

Maguya, A.S., Junttila, V., Kauranne, T., 2013. Adaptive algorithm for large scale dtm interpolation from lidar data for forestry applications in steep forested terrain. ISPRS J. Photogramm. Remote Sens. 85, 74–83.

McCarley, T.R., Hudak, A.T., Sparks, A.M., Vaillant, N.M., Meddens, A.J., Trader, L., Mauro, F., Kreitler, J., Boschetti, L., 2020. Estimating wildfire fuel consumption with multitemporal airborne laser scanning data and demonstrating linkage with MODIS-derived fire radiative energy. Remote Sens. Environ. 251, 112114.

Meng, X., 2005. A slope-and elevation-based filter to remove non-ground measurements from airborne LIDAR data. In: ISPRS WG III/3, III/4, V/3 Workshop "Laserscanning 2005". p. 23.

Meng, X., Currit, N., Zhao, K., 2010. Ground filtering algorithms for airborne LiDAR data: A review of critical issues. Remote Sens. 2 (3), 833–860.

Meng, X., Wang, L., Silván-Cárdenas, J.L., Currit, N., 2009. A multi-directional ground filtering algorithm for airborne LIDAR. ISPRS J. Photogramm. Remote Sens. 64 (1), 117–124.

Mongus, D., Lukač, N., Žalik, B., 2014. Ground and building extraction from LiDAR data based on differential morphological profiles and locally fitted surfaces. ISPRS J. Photogramm. Remote Sens. 93, 145–156.

Mongus, D., Žalik, B., 2012. Parameter-free ground filtering of LiDAR data for automatic DTM generation. ISPRS J. Photogramm. Remote Sens. 67, 1–12.

Mongus, D., Žalik, B., 2014. Computationally efficient method for the generation of a digital terrain model from airborne LiDAR data using connected operators. IEEE J. Sel. Top. Appl. Earth Obs. Remote Sens. 7 (1), 340–351.

Moudry, V., Klapste, P., Fogl, M., Gdulova, K., Bartak, V., Urban, R., 2020. Assessment of LiDAR ground filtering algorithms for determining ground surface of non-natural terrain overgrown with forest and steppe vegetation. Measurement 150, 107047.

Mousa, Y., Helmholz, P., Belton, D., 2017. New DTM extraction approach from airborne images derived DSM. Int. Arch. Photogramm. Remote Sens. Spatial Inf. Sci. XLII-1/W1, 75–82.

Mousa, Y.A., Helmholz, P., Belton, D., Bulatov, D., 2019. Building detection and regularisation using DSM and imagery information. Photogramm. Rec. 34 (165), 85–107.

Muhadi, N.A., Abdullah, A.F., Bejo, S.K., Mahadi, M.R., Mijic, A., 2020. The use of LiDAR-derived DEM in flood applications: A review. Remote Sens. 12 (14), 2308.

Ni, H., Lin, X., Zhang, J., Chen, D., Peethambaran, J., 2018. Joint clusters and iterative graph cuts for ALS point cloud filtering. IEEE J. Sel. Top. Appl. Earth Obs. Remote Sens. 11 (3), 990–1004.

Nie, S., Wang, C., Dong, P., Xi, X., Luo, S., Qin, H., 2017. A revised progressive TIN densification for filtering airborne LiDAR data. Measurement 104, 70–77.

Niemeyer, J., Rottensteiner, F., Soergel, U., 2014. Contextual classification of lidar data and building object detection in urban areas. ISPRS J. Photogramm. Remote Sens. 87, 152–165.

Nurunnabi, A., Geoff, W., Belton, D., 2015. Robust locally weighted regression techniques for ground surface points filtering in mobile laser scanning 3D point cloud data. IEEE Trans. Geosci. Remote Sens. 54, 2181–2193.

Nurunnabi, A., Teferle, F.N., Li, J., Lindenbergh, R.C., Hunegnaw, A., 2021. An efficient deep learning approach for ground point filtering in aerial laser scanning point clouds. Int. Arch. Photogramm. Remote Sens. Spatial Inf. Sci. XLIII-B1-2021, 31–38.

Ortega, S., Trujillo, A., Santana, J.M., Suárez, J.P., Santana, J., 2019. Characterization and modeling of power line corridor elements from LiDAR point clouds. ISPRS J. Photogramm. Remote Sens. 152, 24–33.

Perko, R., Raggam, H., Gutjahr, K., Schardt, M., 2015. Advanced DTM generation from very high resolution satellite stereo images. ISPRS Ann. Photogramm. Remote Sens. Spatial Inf. Sci. II-3/W4, 165–172.

Pfeifer, N., Reiter, T., Briese, C., Rieger, W., 1999. Interpolation of high quality ground models from laser scanner data in forested areas. Int. Arch. Photogramm. Remote Sens. 32, 31–36.

Pfeifer, N., Stadler, P., Briese, C., 2001. Derivation of digital terrain models in the SCOP++ environment. In: Proc. of OEEPE Workshop on Airborne Laserscanning and Interferometric SAR for Detailed Digital Terrain Models, Vol. 3612. http://hdl.handle.net/20.500.12708/43018. (Accessed 7 November 2023).

Pingel, T.J., Clarke, K.C., McBride, W.A., 2013. An improved simple morphological filter for the terrain classification of airborne LIDAR data. ISPRS J. Photogramm. Remote Sens. 77, 21–30.

Qi, C.R., Su, H., Mo, K., Guibas, L.J., 2017a. PointNet: Deep learning on point sets for 3D classification and segmentation. In: Proc. IEEE Conf. Comput. Vis. Pattern Recog. pp. 77–85.

Qi, C.R., Yi, L., Su, H., Guibas, L.J., 2017b. PointNet++: Deep hierarchical feature learning on point sets in a metric space. In: Proc. Adv. Neural Inf. Process. Syst., Vol. 30. pp. 5105–5114.

Qin, N., Hu, X., Dai, H., 2018. Deep fusion of multi-view and multimodal representation of ALS point cloud for 3D terrain scene recognition. ISPRS J. Photogramm. Remote Sens. 143, 205–212.

Qin, N., Tan, W., Ma, L., Zhang, D., Guan, H., Li, J., 2023. Deep learning for filtering the ground from ALS point clouds: A dataset, evaluations and issues. ISPRS J. Photogramm. Remote Sens. 202, 246–261.

Qin, N., Tan, W., Ma, L., Zhang, D., Li, J., 2021. OpenGF: An ultra-large-scale ground filtering dataset built upon open ALS point clouds around the world. In: Proc. IEEE Conf. Comput. Vis. Pattern Recog. Workshops. pp. 1082–1091.

Qin, L., Wu, W., Tian, Y., Xu, W., 2017. LiDAR filtering of urban Areas With Region growing based on moving-window weighted iterative least-squares fitting. IEEE Geosci. Remote. Sens. Lett. 14 (6), 841–845.

Ribeiro, M.T., Singh, S., Guestrin, C., 2016. "Why Should I Trust You?": Explaining the predictions of any classifier. In: Proc. of the 22nd ACM SIGKDD Int. Conf. on Knowledge Discovery and Data Mining. pp. 1135–1144.

Rizaldy, A., Persello, C., Gevaert, C., Oude Elberink, S., Vosselman, G., 2018. Ground and multi-class classification of airborne laser scanner point clouds using fully convolutional networks. Remote Sens. 10 (11), 1723.

Roggero, M., 2001. Airborne laser scanning: Clustering in raw data. Int. Arch. Photogramm. Remote Sens. XXXIV–3/W4, 227–232.
Ros, G., Sellart, L., Materzynska, J., Vazquez, D., Lopez, A.M., 2016. The SYNTHIA dataset: A large collection of synthetic images for semantic segmentation of urban scenes. In: Proc. IEEE Conf. Comput. Vis. Pattern Recog. pp. 3234–3243.
Roynard, X., Deschaud, J.-E., Goulette, F., 2018. Paris-Lille-3D: A large and high-quality ground-truth urban point cloud dataset for automatic segmentation and classification. Int. J. Robot. Res. 37 (6), 545–557.
Schmohl, S., Sörgel, U., 2019. Submanifold sparse convolutional networks for semantic segmentation of large-scale ALS point clouds. ISPRS Ann. Photogramm. Remote Sens. Spatial Inf. Sci. IV-2/W5, 77–84.
Serifoglu Yilmaz, C., Gungor, O., 2018. Comparison of the performances of ground filtering algorithms and DTM generation from a UAV-based point cloud. Geocarto Int. 33, 522–537.
Serifoglu Yilmaz, C., Yilmaz, V., Gungor, O., 2018. Investigating the performances of commercial and non-commercial software for ground filtering of UAV-based point clouds. Int. J. Remote Sens. 39, 5016–5042.
Shan, J., Aparajithan, S., 2005. Urban DEM generation from raw lidar data: A labeling algorithm and its performance. Photogramm. Eng. Remote Sens. 71, 217–226.
Shao, Y.C., Chen, L., 2008. Automated searching of ground points from airborne lidar data using a climbing and sliding method. Photogramm. Eng. Remote Sens. 74, 625–635.
Shelhamer, E., Long, J., Darrell, T., 2017. Fully convolutional networks for semantic segmentation. IEEE Trans. Pattern Anal. Mach. Intell. 39 (4), 640–651.
Shi, X., Ma, H., Chen, Y., Zhang, L., Zhou, W., 2018. A parameter-free progressive TIN densification filtering algorithm for lidar point clouds. Int. J. Remote Sens. 39 (20), 6969–6982.
Silva, C.A., Klauberg, C., Hentz, Â.M.K., Corte, A.P.D., Ribeiro, U., Liesenberg, V., 2018. Comparing the performance of ground filtering algorithms for terrain modeling in a forest environment using airborne LiDAR data. Floresta Ambiente 25 (2), e20160150.
Silván-Cárdenas, J., Wang, L., 2006. A multi-resolution approach for filtering LiDAR altimetry data. ISPRS J. Photogramm. Remote Sens. 61, 11–22.
Simonyan, K., Zisserman, A., 2015. Very deep convolutional networks for large-scale image recognition. In: Proc. Int. Conf. Learn. Represent. https://arxiv.org/pdf/1409.1556.pdf. (Accessed 7 November 2023).
Sithole, G., 2001. Filtering of laser altimetry data using a slope adaptive filter. Int. Arch. Photogramm. Remote Sens. XXXIV-3/W4, 203–210.
Sithole, G., Vosselman, G., 2003. Report: ISPRS comparison of filters. https://www.itc.nl/isprs/wgIII-3/filtertest/report/. (Accessed 7 November 2023).
Sithole, G., Vosselman, G., 2004. Experimental comparison of filter algorithms for bare-earth extraction from airborne laser scanning point clouds. ISPRS J. Photogramm. Remote Sens. 59 (1–2), 85–101.
Sithole, G., Vosselman, G., 2005. Filtering of airborne laser scanner data based on segmented point clouds. In: ISPRS WG III/3, III/4, V/3 Workshop "Laserscanning 2005". pp. 66–71.
Sohn, G., Dowman, I., 2002. Terrain surface reconstruction by the use of tetrahedron model with the MDL criterion. Int. Arch. Photogramm. Remote Sens. XXXIV, 336–344.
Stereńczak, K., Ciesielski, M., Balazy, R., Zawiła-Niedźwiecki, T., 2016. Comparison of various algorithms for DTM interpolation from LIDAR data in dense mountain forests. Eur. J. Remote. Sens. 49 (1), 599–621.
Streutker, D.R., Glenn, N.F., 2006. LiDAR measurement of sagebrush steppe vegetation heights. Remote Sens. Environ. 102 (1), 135–145.
Štroner, M., Urban, R., Lidmila, M., Kolář, V., Křemen, T., 2021. Vegetation filtering of a steep rugged terrain: The performance of standard algorithms and a newly proposed workflow on an example of a railway ledge. Remote Sens. 13, 3050.
Su, W., Sun, Z., Zhong, R., Huang, J., Li, M., Zhu, J., Zhang, K., Wu, H., Zhu, D., 2015. A new hierarchical moving curve-fitting algorithm for filtering lidar data for automatic DTM generation. Int. J. Remote Sens. 36 (14), 3616–3635.
Susaki, J., 2012. Adaptive slope filtering of airborne LiDAR data in urban areas for digital terrain model (DTM) generation. Remote Sens. 4 (6), 1804–1819.
Tan, W., Qin, N., Ma, L., Li, Y., Du, J., Cai, G., Yang, K., Li, J., 2020. Toronto-3D: A large-scale mobile LiDAR dataset for semantic segmentation of urban roadways. In: Proc. IEEE Conf. Comput. Vis. Pattern Recog. Workshops. pp. 797–806.
Thomas, H., Qi, C.R., Deschaud, J.-E., Marcotegui, B., Goulette, F., Guibas, L.J., 2019. KPConv: Flexible and deformable convolution for point clouds. In: Proc. IEEE Int. Conf. Comput. Vis. pp. 6410–6419.
Tóvári, D., Pfeifer, N., 2005. Segmentation based robust interpolation- a new approach to laser data filtering. Int. Arch. Photogramm. Remote Sens. Spat. Inf. Sci. 36, 79–84.
Ural, S., Shan, J., 2016. A min-cut based filter for airborne LIDAR data. Int. Arch. Photogramm. Remote Sens. Spatial Inf. Sci. XLI-B3, 395–401.
Valada, A., Vertens, J., Dhall, A., Burgard, W., 2017. AdapNet: Adaptive semantic segmentation in adverse environmental conditions. In: Int. Conf. on Robotics and Automation. pp. 4644–4651.
Varney, N., Asari, V.K., Graehling, Q., 2020. DALES: A large-scale aerial LiDAR data set for semantic segmentation. In: Proc. IEEE Conf. Comput. Vis. Pattern Recog. Workshops. pp. 186–187.
Vosselman, G., 2000. Slope based filtering of laser altimetry data. Int. Arch. Photogramm. Remote Sens. XXXIII, 935–942.
Wack, R., Wimmer, A., 2002. Digital terrain models from airborne laserscanner data – A grid based approach. Int. Arch. Photogramm. Remote Sens. XXXIV (3/B), 293–296.
Wang, H., Liu, Q., Yue, X., Lasenby, J., Kusner, M.J., 2021. Unsupervised point cloud pre-training via occlusion completion. In: Proc. IEEE Int. Conf. Comput. Vis. pp. 9762–9772.
Wang, Y., Sun, Y., Liu, Z., Sarma, S.E., Bronstein, M.M., Solomon, J.M., 2019. Dynamic graph CNN for learning on point clouds. ACM Trans. Graph. 38 (5), 146.
Wang, C.K., Tseng, Y.H., 2014. Dual-directional profile filter for digital terrain model generation from airborne laser scanning data. J. Appl. Remote. Sens. 8, 083619.
Wang, L., Xu, Y., Li, Y., 2017. Aerial lidar point cloud voxelization with its 3D ground filtering application. Photogramm. Eng. Remote Sens. 83, 95–107.
Wang, T., Zhang, B., Zhang, T., Gu, S., Bao, J., Baltrusaitis, T., Shen, J., Chen, D., Wen, F., Chen, Q., Guo, B., 2023. RODIN: A generative model for sculpting 3D digital avatars using diffusion. In: Proc. IEEE Conf. Comput. Vis. Pattern Recog. pp. 4563–4573.
Xie, S., Gu, J., Guo, D., Qi, C.R., Guibas, L., Litany, O., 2020. PointContrast: Unsupervised pre-training for 3D point cloud understanding. In: Proc. Eur. Conf. Comput. Vis. pp. 574–591.
Yang, B., Huang, R., Dong, Z., Zang, Y., Li, J., 2016. Two-step adaptive extraction method for ground points and breaklines from lidar point clouds. ISPRS J. Photogramm. Remote Sens. 119, 373–389.
Yang, A., Wu, Z., Yang, F., Su, D., Qi, C., 2020. Filtering of airborne LiDAR bathymetry based on bidirectional cloth simulation. ISPRS J. Photogramm. Remote Sens. 163, 49–61.
Ye, Z., Xu, Y., Huang, R., Tong, X., Li, X., Liu, X., Luan, K., Hoegner, L., Stilla, U., 2020. LASDU: A large-scale aerial LiDAR dataset for semantic labeling in Dense Urban Areas. ISPRS Int. J. Geo-Inf. 9 (7), 450.
Yotsumata, T., Sakamoto, M., Satoh, T., 2020. Quality improvement for airborne LIDAR data filtering based on deep learning method. Int. Arch. Photogramm. Remote Sens. Spatial Inf. Sci. XLIII-B2-2020, 355–360.
Yue, X., Wu, B., Seshia, S.A., Keutzer, K., Sangiovanni-Vincentelli, A.L., 2018. A LiDAR point cloud generator: From a virtual world to autonomous driving. In: Proceedings of the 2018 ACM on International Conference on Multimedia Retrieval. pp. 458–464.
Zakšek, K., Pfeifer, N., IAP, Z., 2006. Technical Report: An improved morphological filter for selecting relief points from a LIDAR point cloud in steep areas with dense vegetation. https://iaps.zrc-sazu.si/sites/default/files/Zaksek_Pfeifer_ImprMF.pdf. (Accessed 7 November 2023).
Zeybek, M., Şanlıoğlu, İ., 2019. Point cloud filtering on UAV based point cloud. Measurement 133, 99–111.
Zhang, K., Chen, S.C., Whitman, D., Shyu, M.L., Yan, J., Zhang, C., 2003. A progressive morphological filter for removing nonground measurements from airborne LIDAR data. IEEE Trans. Geosci. Remote Sens. 41 (4), 872–882.
Zhang, Z., Girdhar, R., Joulin, A., Misra, I., 2021. Self-supervised pretraining of 3D features on any point-cloud. In: Proc. IEEE Int. Conf. Comput. Vis. pp. 10232–10243.
Zhang, J., Hu, X., Dai, H., Qu, S., 2020. DEM extraction from ALS point clouds in forest areas via graph convolution network. Remote Sens. 12 (1), 178.
Zhang, J., Lin, X., 2013. Filtering airborne LiDAR data by embedding smoothness-constrained segmentation in progressive TIN densification. ISPRS J. Photogramm. Remote Sens. 81, 44–59.
Zhang, W., Qi, J., Wan, P., Wang, H., Xie, D., Wang, X., Yan, G., 2016. An easy-to-use airborne LiDAR data filtering method based on cloth simulation. Remote Sens. 8 (6), 501.
Zhang, K., Whitman, D., 2005. Comparison of three algorithms for filtering airborne lidar data. Photogramm. Eng. Remote Sens. 71 (3), 313–324.
Zhang, Y., Zhang, Y., Yunjun, Z., Zhao, Z., 2017. A two-step semiglobal filtering approach to extract DTM from middle resolution DSM. IEEE Geosci. Remote Sens. Lett. 14 (9), 1599–1603.
Zhao, X., Guo, Q., Su, Y., Xue, B., 2016. Improved progressive TIN densification filtering algorithm for airborne LiDAR data in forested areas. ISPRS J. Photogramm. Remote Sens. 117, 79–91.
Zhao, X., Su, Y., Li, W., Hu, T., Liu, J., Guo, Q., 2018. A comparison of LiDAR filtering algorithms in Vegetated Mountain Areas. Can. J. Remote Sens. 44 (4), 287–298.
Zheng, S., Shi, W., Liu, J., Zhu, G., 2007. Facet-based airborne light detection and ranging data filtering method. Opt. Eng. 46 (6), 066202.
Zolanvari, S.M.I., Ruano, S., Rana, A., Cummins, A., da Silva, R.E., Rahbar, M., Smolic, A., 2019. DublinCity: Annotated LiDAR point cloud and its applications. In: Proc. British Machine Vis. Conf. https://bmvc2019.org/wp-content/uploads/papers/0644-paper.pdf. (Accessed 7 November 2023).